

# Light dark matter, rare $B$ decays with missing energy in $L_\mu - L_\tau$ model with a scalar leptoquark

Shivaramakrishna Singirala,<sup>1,\*</sup> Suchismita Sahoo,<sup>2,†</sup> and Rukmani Mohanta<sup>1,‡</sup>

<sup>1</sup>School of Physics, University of Hyderabad, Hyderabad-500046, India

<sup>2</sup>Department of Physics, Central University of Karnataka, Kalaburagi-585367, India



(Received 14 June 2021; accepted 6 January 2022; published 31 January 2022)

We investigate the phenomenology of light GeV-scale fermionic dark matter in the  $U(1)_{L_\mu - L_\tau}$  gauge extension of the Standard Model. Heavy neutral fermions alongside with a  $S_1(\bar{3}, 1, 1/3)$  scalar leptoquark and an inert scalar doublet are added to address the flavor anomalies and light neutrino mass respectively. The light gauge boson associated with the  $U(1)_{L_\mu - L_\tau}$  gauge group mediates a dark to visible sector and helps to obtain the correct relic density. Aided with a colored scalar, we constrain the new model parameters by using the branching ratios of various  $b \rightarrow sll$  and  $b \rightarrow s\gamma$  decay processes as well as the lepton flavor nonuniversality observables  $R_{K^{(*)}}$  and then show the implication on the branching ratios of some rare semileptonic  $B \rightarrow (K^{(*)}, \phi) +$  missing energy processes.

DOI: 10.1103/PhysRevD.105.015033

## I. INTRODUCTION

The Standard Model (SM) of particle physics is quite successful in meeting the experimental sensitivities when it comes to interactions at the fundamental level. It is believed to be a low-energy gauge theory embedded in a high-scale unified version. Despite its accomplishments, the increasing sensitivities of various intensity and cosmic frontier experiments have spotlighted its drawbacks and hints toward its extension. Listing a few, there are the existence of dark matter (DM) and its nature [1–6], nonzero neutrino masses and its mixing phenomena [7], matter-antimatter asymmetry [8–12], and so on.

Although most of the flavor observables go along with the SM, there are a collection of recent measurements in semi-leptonic  $B$  meson decays, involving  $b \rightarrow sll$  and  $b \rightarrow c\tau\bar{\nu}_\tau$  quark level transitions, that are incongruous with the SM predictions. The most conspicuous measurements, hinting the physics beyond the SM, are the lepton flavor universality violating parameters:  $R_K$  with a discrepancy of  $3.1\sigma$  [13–17],  $R_{K^{(*)}}$  with a disagreement at the level of  $(2.1 - 2.5)\sigma$  [18,19],  $R_{D^{(*)}}$  with  $3.08\sigma$  discrepancy [20–23], and  $R_{J/\psi}$  with a deviation of nearly  $2\sigma$  [24–26] from their SM predictions. Although the Belle Collaboration [27,28] has also announced their measurements on  $R_{K^{(*)}}$  in various  $q^2$

bins, these measurements have large uncertainties. Besides the  $R_{K^{(*)}}$  parameters, the  $P'_5$  optimized observable disagrees with the SM at the level of  $4\sigma$  in the  $(4.3 - 8.68)$   $\text{GeV}^2$   $q^2$ -bin [29–31] and the decay rate of  $B \rightarrow K^*\mu\mu$  shows  $3\sigma$  discrepancy [32]. The branching ratio of the  $B_s \rightarrow \phi\mu\mu$  channel also disagrees with the theory at the level of  $3\sigma$  [33] in low  $q^2$ .

Because of the above discussed anomalies in  $b \rightarrow sll$ , the rare semileptonic  $B$  decays with charged leptons in the final state such as  $B \rightarrow K^{(*)}ll$ ,  $B_s \rightarrow \phi ll$  have attracted large attention in recent times compared to the analogous semileptonic  $B$  meson channels with neutral leptons in the final state, i.e.,  $B \rightarrow K^{(*)}\nu\bar{\nu}$ ,  $B_s \rightarrow \phi\nu\bar{\nu}$ . Since the neutrinos escape undetected, the number of angular observables associated with charged leptons are also more in contrast to the  $b \rightarrow sv\bar{\nu}$  processes. In the SM, the rare  $b \rightarrow sv\bar{\nu}$  transitions are significantly suppressed by the loop momentum and off-diagonal Cabibbo Kobayashi Maskawa (CKM) matrix elements. Even though these processes are theoretically very clean compared to other flavor changing neutral current (FCNC) decays, these are yet to be observed; there exist only upper limits in the branching ratios of such decays [7]. The theoretical computation of the inclusive  $B \rightarrow X_s\nu\bar{\nu}$  process is quite easy; however, the experimental measurement of this decay is probably unfeasible due to the requirement of reconstruction of all  $X_s$  and the missing neutrinos. However, the exclusive  $B \rightarrow K^{(*)}\nu\bar{\nu}$  processes are more promising to look for physics beyond the SM.

Of particular interest among the FCNC  $B$  decays are the semileptonic decays of the form  $b \rightarrow s + \cancel{E}$ , where  $\cancel{E}$  stands for the missing energy. Besides the production of heavy

\*krishnas542@gmail.com

†suchismita8792@gmail.com

‡rmsp@uohyd.ac.in

Published by the American Physical Society under the terms of the Creative Commons Attribution 4.0 International license. Further distribution of this work must maintain attribution to the author(s) and the published article's title, journal citation, and DOI. Funded by SCOAP<sup>3</sup>.

mesons in charge and  $CP$  correlated states, the existing  $B$ -factories can tag the missing energy decays of  $B$  mesons “on the other side.” In Ref. [34], the leptonic decays of heavy  $B(D)$  mesons to a pair of scalar or fermion or vector particles has been investigated both in a model-independent way and in some popular models. Many new physics models [35–43] also have been proposed to test the observed rates of  $B \rightarrow M + \bar{E}$  decays. Furthermore, the sensitivity of bounds on a weakly interacting massive particle (WIMP)-nucleon cross section for GeV scale dark matter in direct detection experiments is less. This brings us to study a light GeV scale WIMP ( $< 2.5$  GeV) in the light of missing energy in rare  $B$ -decays.

To input our purpose, we opt for a simple but phenomenologically rich  $U(1)_{L_\mu - L_\tau}$  gauge extension that was proposed by He *et al.* in [44,45], and then later explored to explain muon  $g - 2$ , dark matter, neutrino phenomenology, and matter-antimatter asymmetry of the Universe [46–76]. In our previous work [77], we extended this model with three heavy neutral fermions, a  $(\bar{3}, 1, 1/3)$  scalar leptoquark, and investigated heavy fermion DM and various flavor anomalies. In the present work, we look at a low mass regime of DM arising as a missing energy in semileptonic decays of  $B$  mesons to  $M (= K, K^*, \phi)$ . The extant of leptoquark (LQ) is proposed in many theoretical frameworks, such as the grand unified theories [78–81], Pati-Salam model [82–86], quark and lepton composite model [87], and the technicolor model [88,89]. The study of flavor anomalies as well as  $B$  anomalies in connection with the dark matter with scalar LQ have been investigated in the literature [17,77,90–116].

The paper is organized as follows. In Sec. II, we provide the details of model, mixing in gauge, fermion, and scalar sectors. Invisible widths of Higgs and  $Z$  bosons are given in Sec. III. We discuss light dark matter relic density and its detection prospects in Sec. IV. Comments on light neutrino mass are given in Sec. V. Section VI contains a detailed discussion on further constraints on new parameters from the

TABLE I. Fields in the chosen  $U(1)_{L_\mu - L_\tau}$  model.

	Field	$SU(3)_C \times SU(2)_L \times U(1)_Y$	$U(1)_{L_\mu - L_\tau}$	$Z_2$
Fermions	$Q_L \equiv (u, d)_L^T$	$(\mathbf{3}, \mathbf{2}, 1/6)$	0	+
	$u_R$	$(\mathbf{3}, \mathbf{1}, 2/3)$	0	+
	$d_R$	$(\mathbf{3}, \mathbf{1}, -1/3)$	0	+
	$\ell_L \equiv e_L, \mu_L, \tau_L$	$(\mathbf{1}, \mathbf{2}, -1/2)$	$0, 1, -1$	+
	$\ell_R \equiv e_R, \mu_R, \tau_R$	$(\mathbf{1}, \mathbf{1}, -1)$	$0, 1, -1$	+
Scalars	$N_e, N_\mu, N_\tau$	$(\mathbf{1}, \mathbf{1}, 0)$	$0, 1, -1$	-
	$H$	$(\mathbf{1}, \mathbf{2}, 1/2)$	0	+
	$\eta$	$(\mathbf{1}, \mathbf{2}, 1/2)$	0	-
	$\phi_2$	$(\mathbf{1}, \mathbf{1}, 0)$	2	+
Gauge bosons $W_\mu^i$ ( $i = 1, 2, 3$ )	$S_1$	$(\bar{\mathbf{3}}, \mathbf{1}, 1/3)$	-1	-
			0	+
	$B_\mu$	$(\mathbf{1}, \mathbf{1}, 0)$	0	+
	$V_\mu$	$(\mathbf{1}, \mathbf{1}, 0)$	0	+

flavor anomalies. The study of  $B_{(s)} \rightarrow (K^{(*)}, \phi) + \bar{E}$  is presented in Sec. VII. Finally concluding remarks are provided in Sec. VIII.

## II. MODEL DESCRIPTION

We consider a variant of the  $L_\mu - L_\tau$  model [77], recently explored in the context of flavor anomalies and dark matter with three additional neutral fermions  $N_e, N_\mu, N_\tau$  and a  $S_1(\bar{\mathbf{3}}, \mathbf{1}, 1/3)$  scalar leptoquark (SLQ). Alongside, the model is comprised of an additional inert scalar doublet  $\eta$  for generating neutrino mass at one-loop and a singlet  $\phi_2$  that spontaneously breaks the new  $U(1)$  symmetry. The full list of field content is provided in Table I.

The relevant Lagrangian terms corresponding to gauge, fermion, gauge-fermion interaction and scalar sectors are given by

$$\begin{aligned}
\mathcal{L}_G &= -\frac{1}{4}(\hat{\mathbf{W}}_{\mu\nu}\hat{\mathbf{W}}^{\mu\nu} + \hat{B}_{\mu\nu}\hat{B}^{\mu\nu} + \hat{V}_{\mu\nu}\hat{V}^{\mu\nu} + 2\sin\chi\hat{B}_{\mu\nu}\hat{V}^{\mu\nu}), \\
\mathcal{L}_f &= -\frac{1}{2}M_{ee}\overline{N_e^c}N_e - \frac{f_\mu}{2}(\overline{N_\mu^c}N_\mu\phi_2^\dagger + \text{h.c.}) - \frac{f_\tau}{2}(\overline{N_\tau^c}N_\tau\phi_2 + \text{h.c.}) - \frac{1}{2}M_{\mu\tau}(\overline{N_\mu^c}N_\tau + \overline{N_\tau^c}N_\mu), \\
&\quad - \sum_{l=e,\mu,\tau}(Y_{ll}(\overline{\ell_L})_l\tilde{\eta}N_{lR} + \text{h.c.}) - \sum_{q=d,s,b}(y_{qR}\overline{d_{qR}^c}S_1N_\mu + \text{h.c.}), \\
\mathcal{L}_{G-f} &= -g_{\mu\tau}\bar{\mu}\gamma^\mu\mu\hat{V}_\mu + g_{\mu\tau}\bar{\tau}\gamma^\mu\tau\hat{V}_\mu - g_{\mu\tau}\overline{\nu_\mu}\gamma^\mu(1-\gamma^5)\nu_\mu\hat{V}_\mu + g_{\mu\tau}\overline{\nu_\tau}\gamma^\mu(1-\gamma^5)\nu_\tau\hat{V}_\mu \\
&\quad - g_{\mu\tau}\overline{N_\mu^c}\hat{V}_\mu\gamma^\mu\gamma^5N_\mu + g_{\mu\tau}\overline{N_\tau^c}\hat{V}_\mu\gamma^\mu\gamma^5N_\tau, \\
\mathcal{L}_S &= \left| \left( i\partial_\mu - \frac{g}{2}\boldsymbol{\tau}^a \cdot \hat{\mathbf{W}}_\mu^a - \frac{g'}{2}\hat{B}_\mu \right) \eta \right|^2 + \left| \left( i\partial_\mu - \frac{g'}{3}\hat{B}_\mu + g_{\mu\tau}\hat{V}_\mu \right) S_1 \right|^2 + |(i\partial_\mu - 2g_{\mu\tau}\hat{V}_\mu)\phi_2|^2 \\
&\quad - V(H, \eta, \phi_2, S_1),
\end{aligned} \tag{1}$$

where, the scalar potential is expressed as

$$\begin{aligned}
V(H, \eta, \phi_2, S_1) = & \mu_H^2 (H^\dagger H) + \lambda_H (H^\dagger H)^2 + \mu_\eta^2 (\eta^\dagger \eta) \\
& + \lambda_{H\eta} (H^\dagger H)(\eta^\dagger \eta) + \lambda_\eta (\eta^\dagger \eta)^2 \\
& + \lambda'_{H\eta} (H^\dagger \eta)(\eta^\dagger H) \\
& + \frac{\lambda''_{H\eta}}{2} [(H^\dagger \eta)^2 + \text{h.c.}] \\
& + \mu_\phi^2 (\phi_2^\dagger \phi_2) + \lambda_\phi (\phi_2^\dagger \phi_2)^2 \\
& + \mu_S^2 (S_1^\dagger S_1) + \lambda_S (S_1^\dagger S_1)^2 \\
& + [\lambda_{H\phi} (\phi_2^\dagger \phi_2) + \lambda_{HS} (S_1^\dagger S_1)] (H^\dagger H) \\
& + \lambda_{S\phi} (\phi_2^\dagger \phi_2)(S_1^\dagger S_1) + \lambda_{\eta\phi} (\phi_2^\dagger \phi_2)(\eta^\dagger \eta) \\
& + \lambda_{S\eta} (S_1^\dagger S_1)(\eta^\dagger \eta). \tag{2}
\end{aligned}$$

In the above,  $\mu_\phi^2, \mu_H^2 < 0$ , the scalar  $\phi_2$  breaks  $U(1)_{L_\mu - L_\tau}$  spontaneously with  $\langle \phi_2 \rangle = v_2/\sqrt{2}$  and  $SU(2)_L \times U(1)_Y$  gets spontaneously broken by  $H$  with  $\langle H \rangle = v/\sqrt{2}$ . The minimization conditions are as follows:

$$\begin{aligned}
\mu_H^2 &= -\lambda_H v^2 - \lambda_{H\phi} v_2^2/2, \\
\mu_\phi^2 &= -\lambda_\phi v_2^2 - \lambda_{H\phi} v^2/2.
\end{aligned}$$

We have  $\mu_\eta^2, \mu_S^2 > 0$  and the masses of the colored scalar and inert components (charged and neutral) are

$$\begin{aligned}
M_{S_1}^2 &= 2\mu_S^2 + \lambda_{HS} v^2 + \lambda_{S\phi} v_2^2, \\
M_{\eta_c}^2 &= \mu_\eta^2 + \lambda_{H\eta} v^2/2 + \lambda_{\eta\phi} v_2^2/2, \\
M_{\eta_{r,i}}^2 &= \mu_\eta^2 + (\lambda_{H\eta} + \lambda'_{H\eta} \pm \lambda''_{H\eta}) v^2/2 + \lambda_{\eta\phi} v_2^2/2. \tag{3}
\end{aligned}$$

In our analysis, we consider the breaking scale of new  $U(1)$  to be above the electroweak scale. The  $CP$ -odd component of  $\phi_2$  gets absorbed by the new  $U(1)$  associated gauge boson, which plays a major role in the subsequent phenomenological study. The mass of the colored scalar is taken to be 1.2 TeV.<sup>1</sup>

### A. Gauge mixing

For the mixing of the gauge bosons of  $U(1)_Y$  and  $U(1)_{L_\mu - L_\tau}$  symmetries, we use the transformation [118]

<sup>1</sup>The most relevant process for the SLQ search at the LHC is the pair production through  $gg(q\bar{q}) \rightarrow S_1^\dagger S_1$ . Both ATLAS and CMS have searched for this production process through different LQ decay channels into second and third generation quarks and leptons:  $S_1^\dagger S_1 \rightarrow t\bar{t}\ell\bar{\ell}, b\bar{b}\nu\bar{\nu}$ . As a consequence, these searches provide suitable model-independent constraints both on mass and branching fractions of the LQ. The best limits on the masses of second/third generation LQs obtained for benchmark branching ratio values set to  $\beta' = 1(0.5)$  are as follows: 900(560) GeV from  $t\bar{t}\tau\bar{\tau}$  and 1100(800) GeV from  $b\bar{b}\nu\bar{\nu}$  channels [117].

$$\begin{pmatrix} \bar{B}_\mu \\ \bar{V}_\mu \end{pmatrix} = \begin{pmatrix} 1 & \sin\chi \\ 0 & \cos\chi \end{pmatrix} \begin{pmatrix} \hat{B}_\mu \\ \hat{V}_\mu \end{pmatrix}. \tag{4}$$

Thus, the gauge kinetic terms take canonical form,

$$\mathcal{L}'_G = -\frac{1}{4} (\hat{W}_{\mu\nu} \hat{W}^{\mu\nu} + \bar{B}_{\mu\nu} \bar{B}^{\mu\nu} + \bar{V}_{\mu\nu} \bar{V}^{\mu\nu}). \tag{5}$$

Expanding the scalar covariant derivatives, we obtain the mass matrix of gauge fields in the basis  $(W_\mu^3, \bar{B}_\mu, \bar{V}_\mu)$  as

$$M_G^2 = \begin{pmatrix} \frac{1}{8}g^2 v^2 & -\frac{1}{8}gg'v^2 & \frac{1}{8}gg'\tan\chi v^2 \\ -\frac{1}{8}gg'v^2 & \frac{1}{8}g'^2 v^2 & -\frac{1}{8}g'^2\tan\chi v^2 \\ \frac{1}{8}gg'\tan\chi v^2 & -\frac{1}{8}g'^2\tan\chi v^2 & 2g_{\mu\tau}^2 \sec\chi^2 v^2 \end{pmatrix}. \tag{6}$$

Two unitary matrices are required to get to the mass eigenstate basis of gauge bosons, given as follows:

$$\begin{aligned}
U_1^T M_G^2 U_1 &= \frac{1}{2} \begin{pmatrix} M_{Z_{\text{SM}}}^2 & 0 & \delta M^2 \\ 0 & 0 & 0 \\ \delta M^2 & 0 & M_V^2 \end{pmatrix} \quad \text{with} \\
U_1 &= \begin{pmatrix} \cos\theta_w & \sin\theta_w & 0 \\ -\sin\theta_w & \cos\theta_w & 0 \\ 0 & 0 & 1 \end{pmatrix}. \tag{7}
\end{aligned}$$

In the above,

$$\begin{aligned}
M_{Z_{\text{SM}}}^2 &= \frac{1}{4}(g^2 + g'^2)v^2, \\
M_V^2 &= 4g_{\mu\tau}^2 \sec\chi^2 v_2^2, \\
\delta M^2 &= \frac{1}{4}g' \sqrt{(g^2 + g'^2)} \tan\chi v^2, \\
\theta_w &= \tan^{-1}[g'/g]. \tag{8}
\end{aligned}$$

Further operating with  $U_2$ , we obtain

$$\begin{aligned}
(U_1 U_2)^T M_G^2 (U_1 U_2) &= \frac{1}{2} \begin{pmatrix} M_Z^2 & 0 & 0 \\ 0 & 0 & 0 \\ 0 & 0 & M_{Z'}^2 \end{pmatrix} \quad \text{with} \\
U_2 &= \begin{pmatrix} \cos\alpha & 0 & \sin\alpha \\ 0 & 1 & 0 \\ -\sin\alpha & 0 & \cos\alpha \end{pmatrix}, \tag{9}
\end{aligned}$$

The masses of physical gauge fields and corresponding mixing angle read as

TABLE II. Model parameters along with their values in the present model.

Parameters	$M_{S_1}$ [GeV]	$M_+$ [GeV]	$M_{H_1}$ [GeV]	$M_{H_2}$ [GeV]	$\sin\beta$	$\sin\zeta$	$\chi$	$\alpha \times 10^4$
Values	1200	500	125	500	1/2	$10^{-3} - 10^{-2}$	$10^{-3}$	4.83–4.85

$$\begin{aligned} M_Z^2 &= M_{Z_{\text{SM}}}^2 \cos\alpha^2 - \delta M^2 \sin 2\alpha + M_V^2 \sin\alpha^2, \\ M_{Z'}^2 &= M_{Z_{\text{SM}}}^2 \sin\alpha^2 + \delta M^2 \sin 2\alpha + M_V^2 \cos\alpha^2, \\ \alpha &= \frac{1}{2} \tan^{-1} \left[ \frac{2\delta M^2}{M_V^2 - M_{Z_{\text{SM}}}^2} \right]. \end{aligned} \quad (10)$$

Thus, the gauge and mass eigenstates can be related by

$$\begin{pmatrix} \hat{W}_\mu^3 \\ \bar{B}_\mu \\ \bar{V}_\mu \end{pmatrix} = U_1 U_2 \begin{pmatrix} Z_\mu \\ A_\mu \\ Z'_\mu \end{pmatrix}. \quad (11)$$

In the low-mass regime of  $Z'$ , the kinetic mixing gets severely constrained ( $\chi \sim 10^{-3}$ ) from electroweak precision data [119,120], and the mixing angle  $\alpha \sim 4.84 \times 10^{-4}$ .

Bounds on the new gauge parameters ( $M_{Z'}$  and  $g_{\mu\tau}$ ) are levied by various collider experiments. Upper limits are provided by *BABAR* [121] from the cross section of  $\sigma(e^+e^- \rightarrow \mu^+\mu^-Z', Z' \rightarrow \mu^+\mu^-)$  and also from *CMS* [122] from the process  $p p \rightarrow Z\mu\mu, Z \rightarrow Z'\mu\mu$  going to a  $4\mu$  final state. Other bounds from *Belle* [123] are from the invisible decays of  $Z'$  as missing energy in  $e^+e^-$  collisions. Stringent limits are provided from the study of neutrino trident production from CCFR Collaboration [124,125] and DUNE [66].

### B. Scalar and Fermion mixing

The  $CP$ -even scalars ( $h$  and  $h_2$ ) and also the heavy fermion states ( $N_\mu$  and  $N_\tau$ ) mix with each other. The mixing matrices of both scalar and fermion sectors are given by

$$\begin{aligned} M_H^2 &= \begin{pmatrix} 2\lambda_H v^2 & \lambda_{H\phi} v v_2 \\ \lambda_{H\phi} v v_2 & 2\lambda_\phi v_2^2 \end{pmatrix}, \\ M_N &= \begin{pmatrix} \frac{1}{\sqrt{2}} f_\mu v_2 & M_{\mu\tau} \\ M_{\mu\tau} & \frac{1}{\sqrt{2}} f_\tau v_2 \end{pmatrix}. \end{aligned} \quad (12)$$

One can diagonalize the above mass matrices as follows:  $U_\beta^T M_N U_\beta = \text{diag}[M_-, M_+]$  and  $U_\zeta^T M_H^2 U_\zeta = \text{diag}[M_{H_1}^2, M_{H_2}^2]$ , where  $U_{\beta(\zeta)}$  are  $2 \times 2$  unitary matrix. The mixing angles read as  $\zeta = \frac{1}{2} \tan^{-1} \left( \frac{\lambda_{H\phi} v v_2}{\lambda_\phi v_2^2 - \lambda_H v^2} \right)$  and  $\beta = \frac{1}{2} \tan^{-1} \left( \frac{2M_{\mu\tau}}{(f_\tau - f_\mu)(v_2/\sqrt{2})} \right)$ . The couplings and mass eigenvalues are related as

$$\begin{aligned} f_\mu &= \frac{\sqrt{2}}{v_2} (M_- \cos^2 \beta + M_+ \sin^2 \beta), \\ f_\tau &= \frac{\sqrt{2}}{v_2} (M_- \sin^2 \beta + M_+ \cos^2 \beta), \\ M_{\mu\tau} &= \cos \beta \sin \beta (M_+ - M_-), \\ \lambda_H &= \frac{1}{2v^2} (M_{H_1}^2 \cos^2 \zeta + M_{H_2}^2 \sin^2 \zeta), \\ \lambda_\phi &= \frac{1}{2v_2^2} (M_{H_1}^2 \sin^2 \zeta + M_{H_2}^2 \cos^2 \zeta), \\ \lambda_{H\phi} &= \frac{1}{vv_2} \cos \zeta \sin \zeta (M_{H_2}^2 - M_{H_1}^2). \end{aligned} \quad (13)$$

In case of a scalar sector with minimal mixing ( $\sin\zeta < 10^{-2}$ ), the mass eigenstate  $H_1$  is assumed to be an observed Higgs boson at the LHC ( $M_{H_1} \sim 125$  GeV) and  $H_2$  is considered to be a heavier one with mass 500 GeV. In the fermion spectrum,  $N_-$  is the stable light dark matter with mass less than 2.5 GeV and  $M_+ = 500$  GeV, with the corresponding mixing parameter  $\sin\beta = 1/2$ . All the mentioned values for model parameters are provided in Table II, which will be utilized for the analysis in the subsequent sections.

### III. INVISIBLE WIDTHS

In the present work, Higgs ( $H_1$ ) and  $Z$  bosons can decay to  $N_- N_-$  and the corresponding expressions for invisible widths are given as follows:

$$\Gamma_{\text{inv}}^{H_1} = \frac{(f_\mu \cos^2 \beta + f_\tau \sin^2 \beta)^2 \sin^2 \zeta}{8\pi} M_{H_1} \left( 1 - \frac{4M_-^2}{M_{H_1}^2} \right)^{\frac{3}{2}}. \quad (14)$$

$$\Gamma_{\text{inv}}^Z = \Gamma_{\nu\bar{\nu}}^Z + \Gamma_{N_- N_-}^Z, \text{ where}$$

$$\begin{aligned} \Gamma_{\nu\bar{\nu}}^Z &= \frac{g^2 (\cos \alpha - \sin \alpha \tan \chi \sin \theta_w)^2}{96\pi \cos^2 \theta_w} M_Z, \\ \Gamma_{N_- N_-}^Z &= \frac{(g_{\mu\tau} \cos 2\beta \sec \chi \sin \alpha)^2}{24\pi} M_Z \left( 1 - \frac{4M_-^2}{M_Z^2} \right)^{\frac{3}{2}}. \end{aligned} \quad (15)$$

Figure 1 projects the above widths as a function of  $N_-$  mass.

### IV. DARK MATTER

#### A. Abundance

To compute the relic density of the light DM ( $N_-$ ) via a freeze-out mechanism, we use LanHEP [126] and

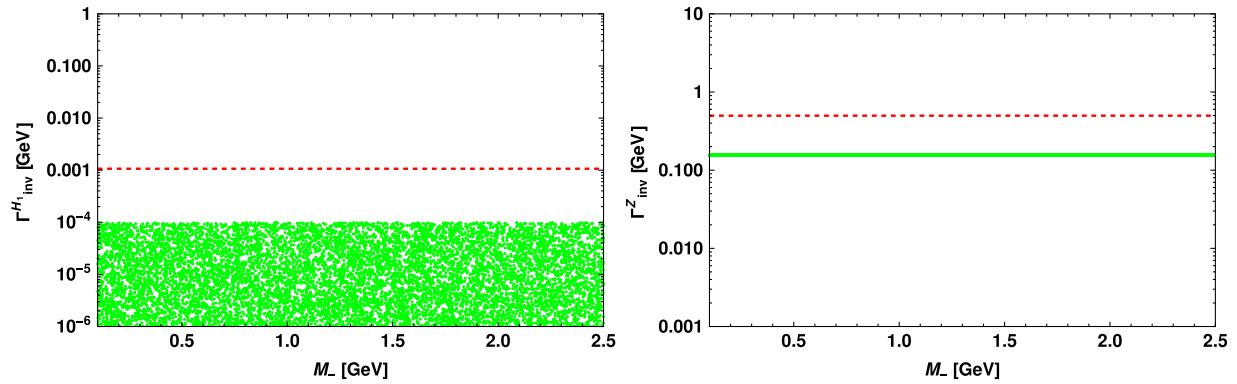


FIG. 1. Left: projection of invisible width of Higgs ( $H_1$ ) for  $\sin \zeta < 10^{-2}$ . Right: projection of the same for Z boson. Corresponding experimental upper limits [131,132] are denoted by red horizontal dashed lines.

micrOMEGAs packages [127–129]. The channels with a lepton-antilepton pair in a final state ( $\mu\bar{\mu}, \tau\bar{\tau}, \nu_\mu\bar{\nu}_\mu, \nu_\tau\bar{\nu}_\tau$ ) via  $Z'$  and  $\eta$  portals contribute to relic density. Furthermore, SLQ portal  $t$ -channel processes with  $d\bar{d}, s\bar{s}$  in the final state are also kinematically allowed. The key point is that the  $s$ -channel processes via light  $Z'$  provide a resonance in propagator, thereby meeting the Planck relic density value [130] for the DM mass in the range 0.1–2.5 GeV. The same is visible from the left panel of Fig. 2, which projects relic density of DM with its mass. The right panel shows the  $3\sigma$  Planck allowed region in the  $M_{Z'}$ - $M_-$  plane.

## B. Detection prospects

Moving to a detection paradigm, a SLQ portal spin-dependent (SD) cross section can arise from the effective interaction

$$\mathcal{L}_{\text{eff}}^{\text{SD}} \simeq \frac{y_{qR}^2 \cos^2 \beta}{4(M_{S_1}^2 - M_-^2)} \overline{N_-} \gamma^\mu \gamma^5 N_- \bar{q} \gamma_\mu \gamma^5 q. \quad (16)$$

The computed cross section is given by [133]

$$\sigma_{\text{SD}} = \frac{\mu_r^2}{\pi} \frac{\cos^4 \beta}{(M_{S_1}^2 - M_-^2)^2} [y_{dR}^2 \Delta_d + y_{sR}^2 \Delta_s]^2 J_n(J_n + 1), \quad (17)$$

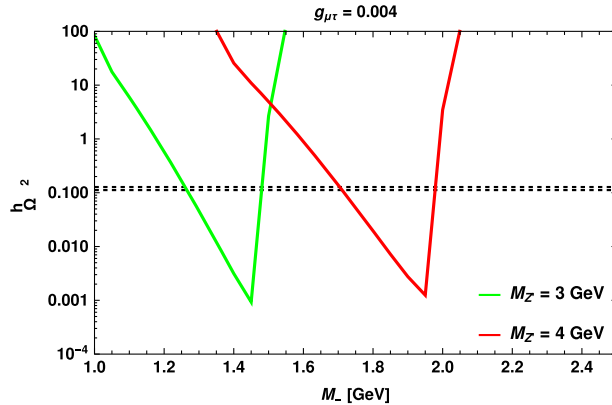


FIG. 2. Behavior of relic density plotted against DM mass with black horizontal dotted lines denoting the  $3\sigma$  range of the Planck limit [130]. The right panel corresponds to the parameter space consistent with the  $3\sigma$  allowed region of Planck data.

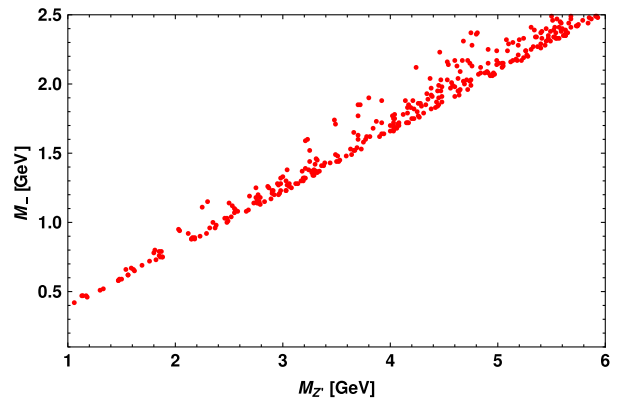
where  $J_n = \frac{1}{2}$  stands for angular momentum,  $\mu_r$  represents the reduced mass, and the values of quark spin functions  $\Delta_q$  are provided in [133]. Figure 3 projects the SD cross section and it is clear that it is well below the experimental upper limit from CDMSlite [134]. Furthermore, the WIMP-nucleon cross section in the gauge portal (via  $Z, Z'$ ) and the scalar portal (via  $H_1, H_2$ ) is found to be very small and insensitive to direct detection experiments.

## V. BRIEF COMMENTS ON NEUTRINO MASS

Neutrino mass can be obtained at one-loop level from the Yukawa interaction with  $\eta$  in Eq. (1). Assuming  $(M_{\eta_r}^2 + M_{\eta_i}^2)/2 = m_0^2$  is much greater than  $M_{\eta_r}^2 - M_{\eta_i}^2 = \lambda''_{H\eta} v^2$ , the expression for the radiatively generated neutrino mass [135,136] is given by

$$(\mathcal{M}_\nu)_{\beta\gamma} = \frac{\lambda''_{H\eta} v^2}{32\pi^2} \sum_{i=1}^3 \frac{Y_{\beta i} Y_{\gamma i}}{M_{ii}^2} \left[ \frac{M_{ii}^2}{m_0^2 - M_{ii}^2} + \frac{M_{ii}^4}{(m_0^2 - M_{ii}^2)^2} \ln \frac{M_{ii}^2}{m_0^2} \right], \quad (18)$$

where  $M_{ij} = \text{diag}(M_{ee}, M_-, M_+)$ . For  $m_0 \sim 1$  TeV,  $\lambda_5 \sim 10^{-1}$  and  $Y \sim 10^{-4}$ , one can obtain neutrino mass at sub-eV



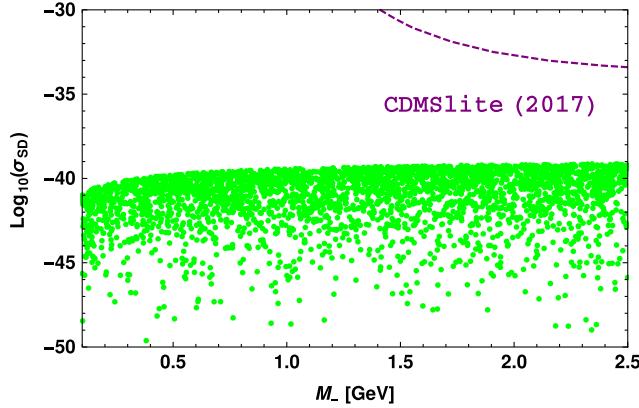


FIG. 3. Spin-dependent WIMP-proton cross section as a function of DM mass in a SLQ portal. Dashed line represents the bound levied by CDMSlite [134].

scale. It should be noted that as the  $L_\mu - L_\tau$  charges of SM leptons and the heavy fermions are the same for each generation while the inert doublet is charged zero, the Yukawa matrix  $Y$  is diagonal. Hence, the neutrino mass matrix (18) is diagonal by model construction, i.e.,  $\mathcal{M}_\nu = \text{diag}(m_1, m_2, m_3)$ , thus it can automatically accommodate the observed neutrino mixing angles, i.e., any unitary matrix can be used as the neutrino mixing matrix.

## VI. CONSTRAINTS ON NEW PARAMETERS FROM THE FLAVOR SECTOR

Now, we look forward to constraining the model parameters of LQ and  $Z'$  couplings using the branching ratios of  $B \rightarrow K\mu\mu$ ,  $B \rightarrow K^*\mu\mu$ ,  $B \rightarrow X_s\gamma$  decay modes and the recent measurements on lepton nonuniversality parameters,  $R_{K^{(*)}}$ .

### A. $b \rightarrow sll$

The general effective Hamiltonian mediating the  $b \rightarrow sl^+l^-$  transition is given by [137,138]

$$\mathcal{H}_{\text{eff}} = -\frac{4G_F}{\sqrt{2}} V_{tb} V_{ts}^* \left[ \sum_{i=1}^6 C_i(\mu) O_i + \sum_{i=7,9,10} (C_i(\mu) O_i + C'_i(\mu) O'_i) \right], \quad (19)$$

where  $G_F$  is the Fermi constant,  $V_{qq'}$  denote the CKM matrix elements,  $C_i$ 's stand for the Wilson coefficients evaluated at the renormalized scale  $\mu = m_b$  [139], and the

TABLE III. The SM Wilson coefficients computed at the scale  $\mu = 4.6$  GeV [139].

$C_1$	$C_2$	$C_3$	$C_4$	$C_5$	$C_6$	$C_7^{\text{eff}}$	$C_8^{\text{eff}}$	$C_9$	$C_{10}$
-3.001	1.008	-0.0047	-0.0827	0.0003	0.0009	-0.2969	-0.1642	4.2607	-4.2453

values at next-to-leading logarithmic ( $C_{9,10}$  values are calculated in the next-to-next-to-leading logarithmic order) are listed in Table III.

Here  $O_i$ 's represent dimension-six operators responsible for leptonic/semileptonic processes, given as

$$\begin{aligned} O_7^{(\prime)} &= \frac{e}{16\pi^2} [\bar{s}\sigma_{\mu\nu}(m_s P_{L(R)} + m_b P_{R(L)})b] F^{\mu\nu}, \\ O_9^{(\prime)} &= \frac{\alpha_{\text{em}}}{4\pi} (\bar{s}\gamma^\mu P_{L(R)} b)(\bar{l}\gamma_\mu l), \\ O_{10}^{(\prime)} &= \frac{\alpha_{\text{em}}}{4\pi} (\bar{s}\gamma^\mu P_{L(R)} b)(\bar{l}\gamma_\mu \gamma_5 l), \end{aligned} \quad (20)$$

where  $\alpha_{\text{em}}$  is the fine-structure constant,  $P_{L,R} = (1 \mp \gamma_5)/2$  are the chiral operators, and the values of primed Wilson coefficient are zero in the SM, but can be nonzero in the proposed  $L_\mu - L_\tau$  model.

The one-loop diagrams that provide nonzero contribution to the rare  $b \rightarrow sll$  processes can take place via the exchange of  $Z'$ ,  $H_{1,2}$  one-loop penguin diagrams with SLQ and  $N_\pm$  particles inside the loop as shown in Fig. 4. The loop functions of second and third diagrams have  $m_q M_\pm/M_{S_1}^2$  factor suppression, hence provide minimal contribution to  $b \rightarrow sll$  processes. Thus, only the first diagram, mediated via  $s$   $Z'$  boson will contribute significantly to the  $b \rightarrow sll$  channels.

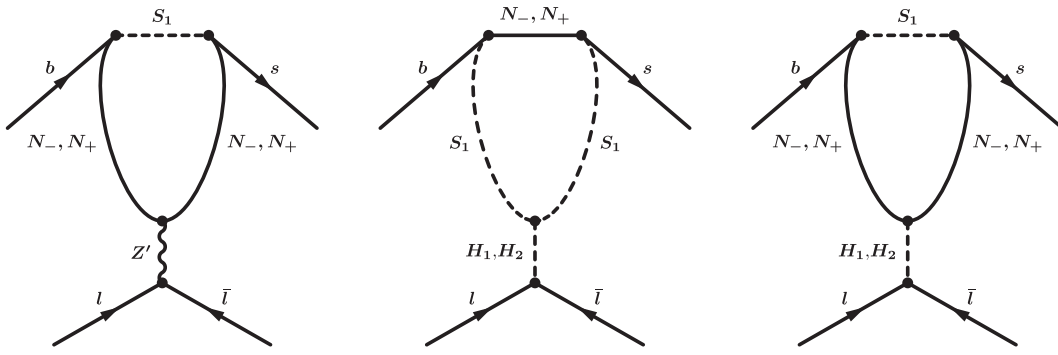
In the presence of a  $Z'$  exchanging one-loop diagram, the transition amplitude of semileptonic  $b \rightarrow sll$  decay process is given by [77]

$$\begin{aligned} \mathcal{M} &= \frac{1}{2^5 \pi^2} \frac{y_{qR}^2 g_{\mu\tau}^2}{(q^2 - M_{Z'}^2)} \mathcal{V}_{sb}(\chi_-, \chi_+) \\ &\times [\bar{u}(p_B)\gamma^\mu(1 + \gamma_5)u(p_K)][\bar{v}(p_2)\gamma_\mu u(p_1)], \end{aligned} \quad (21)$$

which in comparison with the generalized effective Hamiltonian provides additional primed Wilson coefficient [77]

$$C_9^{\text{NP}} = \frac{\sqrt{2}}{2^4 \pi G_F \alpha_{\text{em}} V_{tb} V_{ts}^*} \frac{y_{qR}^2 g_{\mu\tau}^2}{(q^2 - M_{Z'}^2)} \mathcal{V}_{sb}(\chi_-, \chi_+), \quad (22)$$

to  $b \rightarrow sll$  process. Here  $p_B$ ,  $p_K$ , and  $p_{1,2}$  are the four momenta of the initial  $B$  meson, final  $K$  meson, and the charged leptons, respectively. The detailed expression for the loop function  $\mathcal{V}_{sb}(\chi_-, \chi_+)$  with  $\chi_\pm = M_\pm^2/M_{S_1}^2$  is given in the Appendix A [58,140]. Since there is only  $C_9^{\text{NP}}$  in this model, the  $B_s \rightarrow \mu\mu(\tau\tau)$  will not play any role in constraining the new parameters.

FIG. 4. One-loop penguin diagrams that provide nonzero contribution to  $b \rightarrow sll$  transitions in the present model.**1.  $B \rightarrow Kl^+l^-$** 

Including the new physics contribution, the differential branching ratio of  $B \rightarrow Kll$  process in terms of  $q^2$  is given by [16]

$$\frac{d\text{Br}}{dq^2} = \tau_B \frac{G_F^2 \alpha_{\text{em}}^2 |V_{tb} V_{ts}^*|^2}{2^8 \pi^5 M_B^3} \sqrt{\lambda(M_B^2, M_K^2, q^2)} \beta_l f_+^2 \\ \times \left( a_l(q^2) + \frac{c_l(q^2)}{3} \right), \quad (23)$$

where

$$a_l(q^2) = q^2 |F_P|^2 + \frac{\lambda(M_B^2, M_K^2, q^2)}{4} (|F_A|^2 + |F_V|^2) \\ + 2m_l(M_B^2 - M_K^2 + q^2) \text{Re}(F_P F_A^*) + 4m_l^2 M_B^2 |F_A|^2, \\ c_l(q^2) = -\frac{\lambda(M_B^2, M_K^2, q^2)}{4} \beta_l^2 (|F_A|^2 + |F_V|^2), \quad (24)$$

with

$$F_V = \frac{2m_b}{M_B} C_7^{\text{eff}} + C_9^{\text{eff}} + C_9^{\text{NP}}, \quad F_A = C_{10}^{\text{SM}}, \\ F_P = m_l C_{10}^{\text{SM}} \left[ \frac{M_B^2 - M_K^2}{q^2} \left( \frac{f_0(q^2)}{f_+(q^2)} - 1 \right) - 1 \right], \quad (25)$$

and

$$\lambda(a, b, c) = a^2 + b^2 + c^2 - 2(ab + bc + ca), \\ \beta_l = \sqrt{1 - 4m_l^2/q^2}. \quad (26)$$

The detailed expression for  $C_{7,9}^{\text{eff}}$  Wilson coefficients [141–143] is presented in Appendix C. By using the lifetime of a  $B$  meson and masses of all the particles from [7], the  $B \rightarrow K$  form factors from [144] and the predicted branching ratio values of  $B \rightarrow K\mu\mu(\tau\tau)$  processes are

$$\text{Br}(B^0 \rightarrow K^0 \mu^+ \mu^-)|^{\text{SM}} = (1.48 \pm 0.12) \times 10^{-7}, \quad (27)$$

$$\text{Br}(B^+ \rightarrow K^+ \mu^+ \mu^-)|^{\text{SM}} = (1.6 \pm 0.13) \times 10^{-7}, \quad (28)$$

$$\text{Br}(B^+ \rightarrow K^+ \tau^+ \tau^-)|^{\text{SM}} = (1.52 \pm 0.121) \times 10^{-7}, \quad (29)$$

which in comparison with the corresponding experimental data [7]

$$\text{Br}(B^0 \rightarrow K^0 \mu^+ \mu^-)|^{\text{Expt}} = (3.39 \pm 0.34) \times 10^{-7}, \quad (30)$$

$$\text{Br}(B^+ \rightarrow K^+ \mu^+ \mu^-)|^{\text{Expt}} = (4.41 \pm 0.22) \times 10^{-7}, \quad (31)$$

$$\text{Br}(B^+ \rightarrow K^+ \tau^+ \tau^-)|^{\text{Expt}} < 2.25 \times 10^{-3}, \quad (32)$$

can put constraints on  $y_{qR}$ ,  $g_{\mu\tau}$ ,  $M_-$ , and  $M_{Z'}$  parameters. As  $Z'$  does not couple to electrons, here we have considered only the channels with  $\mu$  and  $\tau$  in the final state.

**2.  $B \rightarrow K^* l^+ l^-$** 

The dilepton invariant mass spectrum for  $B \rightarrow K^* l^+ l^-$  decays after integration over all angles;  $\theta_l$  (angle between  $l^-$  and  $B$  in the dilepton frame),  $\theta_{K^*}$  (angle between  $K^-$  and  $B$  in the  $K^-\pi^+$  frame), and  $\phi$  (angle between the normal of the  $K^-\pi^+$  and the dilepton planes) [145] is given by

$$\frac{d\Gamma}{dq^2} = \frac{3}{4} \left( J_1 - \frac{J_2}{3} \right), \quad J_{1,2} = 2J_{1,2}^s + J_{1,2}^c, \quad (33)$$

where the detailed expressions for  $J_{1,2}^{s(c)}$  as a function of transversity amplitudes are given as [146]

$$\begin{aligned}
J_1^s &= \frac{(2 + \beta_l^2)}{4} [|A_{\perp}^L|^2 + |A_{\parallel}^L|^2 + (L \rightarrow R)] \\
&\quad + \frac{4m_l^2}{q^2} \text{Re}(A_{\perp}^L A_{\perp}^{R*} + A_{\parallel}^L A_{\parallel}^{R*}), \\
J_1^c &= |A_0^L|^2 + |A_0^R|^2 + \frac{4m_l^2}{q^2} [|A_t|^2 + 2\text{Re}(A_0^L A_0^{R*})], \\
J_2^s &= \frac{\beta_l^2}{4} [|A_{\perp}^L|^2 + |A_{\parallel}^L|^2 + (L \rightarrow R)], \\
J_2^c &= -\beta_l^2 [|A_0^L|^2 + (L \rightarrow R)], 
\end{aligned} \tag{34}$$

with

$$A_i A_j^* = A_i^L(q^2) A_j^{*L}(q^2) + A_i^R(q^2) A_j^{*R}(q^2) \quad (i, j = 0, \parallel, \perp), \tag{35}$$

in shorthand notation. The transversity amplitudes in terms of the form factors and (new) Wilson coefficients are given as [146]

$$\begin{aligned}
A_{\perp L,R} &= N \sqrt{2\lambda(M_{K^*}^2, M_B^2, q^2)} \left[ ((C_9^{\text{eff}} + C_9^{\text{NP}}) \mp C_{10}^{\text{SM}}) \frac{V(q^2)}{M_B + M_{K^*}} + \frac{2m_b}{q^2} C_7 T_1(q^2) \right], \\
A_{\parallel L,R} &= -N \sqrt{2}(M_B^2 - M_{K^*}^2) \left[ ((C_9^{\text{eff}} - C_9^{\text{NP}}) \mp C_{10}^{\text{SM}}) \frac{A_1(q^2)}{M_B - M_{K^*}} + \frac{2m_b}{q^2} C_7 T_2(q^2) \right], \\
A_{0L,R} &= -\frac{N}{2M_{K^*}\sqrt{s}} \left[ (C_9^{\text{eff}} - C_9^{\text{NP}}) \mp C_{10}^{\text{SM}} \right. \\
&\quad \times \left. \left( (M_B^2 - M_{K^*}^2 - q^2)(M_B + M_{K^*}) A_1(q^2) - \lambda(M_{K^*}^2, M_B^2, q^2) \frac{A_2(q^2)}{M_B + M_{K^*}} \right) \right. \\
&\quad \left. + 2M_B C_7 \left( (M_B^2 + 3M_{K^*}^2 - q^2) T_2(q^2) - \frac{\lambda(M_{K^*}^2, M_B^2, q^2)}{M_B^2 - M_{K^*}^2} \right) \right], \\
A_t &= 2N \sqrt{\frac{\lambda(M_{K^*}^2, M_B^2, q^2)}{q^2}} C_{10}^{\text{SM}} A_0(q^2),
\end{aligned} \tag{36}$$

where

$$N = V_{tb} V_{ts}^* \left[ \frac{G_F^2 \alpha_{\text{em}}^2}{3 \cdot 2^{10} \pi^5 M_B^3} q^2 \beta_l \sqrt{\lambda(M_{K^*}^2, M_B^2, q^2)} \right]^{1/2}. \tag{37}$$

With the use of the mass and lifetime of particles from the Particle Data Group [7] and the form factor from [147], the predicted branching ratios of  $B \rightarrow K^* \mu \mu (\tau \tau)$  are

$$\text{Br}(B^0 \rightarrow K^{*0} \mu^+ \mu^-)|^{\text{SM}} = (1.967 \pm 0.158) \times 10^{-8}, \tag{38}$$

$$\text{Br}(B^+ \rightarrow K^{*+} \mu^+ \mu^-)|^{\text{SM}} = (1.758 \pm 0.141) \times 10^{-8}, \tag{39}$$

which in correlation with the corresponding experimental data [7]

$$\text{Br}(B^0 \rightarrow K^{*0} \mu^+ \mu^-)|^{\text{Expt}} = (9.4 \pm 0.5) \times 10^{-7}, \tag{40}$$

$$\text{Br}(B^+ \rightarrow K^{*+} \mu^+ \mu^-)|^{\text{Expt}} < 5.9 \times 10^{-7}, \tag{41}$$

can constrain the  $y_{qR}$ ,  $g_{\mu\tau}$ ,  $M_-$ , and  $M_{Z'}$  parameters.

### 3. $R_{K^{(*)}}$

Using the full Run-I and Run-II dataset, recently the LHCb Collaboration has updated the lepton nonuniversality  $R_K$  parameter in the  $q^2 \in [1, 6]$  GeV $^2$  [15]

$$R_K^{\text{LHCb21}} = \frac{\text{Br}(B^+ \rightarrow K^+ \mu^+ \mu^-)}{\text{Br}(B^+ \rightarrow K^+ e^+ e^-)} = 0.846^{+0.042+0.013}_{-0.039-0.012} \tag{42}$$

which is pretty much more precise than the previous result [14]

$$R_K^{\text{LHCb19}} = 0.846^{+0.060+0.016}_{-0.054-0.014} \tag{43}$$

(where the first uncertainty is statistical and the second one is systematic), giving rise to the disagreement of  $3.1\sigma$  from the SM prediction [16,17]

$$R_K^{\text{SM}} = 1.0003 \pm 0.0001. \tag{44}$$

Equivalently, the recent measurements by the LHCb experiment on  $R_{K^*}$  ratio in two bins of low- $q^2$  regions [18]

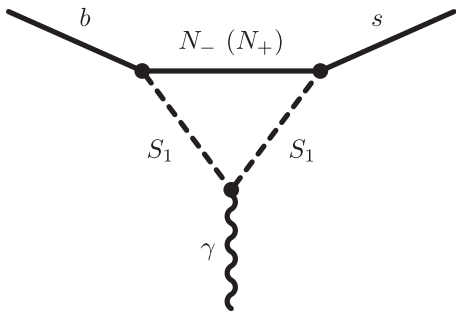


FIG. 5. One-loop diagram of  $b \rightarrow s\gamma$  processes in the proposed model.

$$R_{K^*}^{\text{LHCb}} = \begin{cases} 0.660^{+0.110}_{-0.070} \pm 0.03 & q^2 \in [0.045, 1.1] \text{ GeV}^2, \\ 0.69^{+0.11}_{-0.07} \pm 0.05 & q^2 \in [1.1, 6.0] \text{ GeV}^2. \end{cases} \quad (45)$$

have respectively  $2.1\sigma$  and  $2.5\sigma$  deviations from their corresponding SM values [19]:

$$R_{K^*}^{\text{SM}} = \begin{cases} 0.92 \pm 0.02 & q^2 \in [0.045, 1.1] \text{ GeV}^2, \\ 1.00 \pm 0.01 & q^2 \in [1.1, 6.0] \text{ GeV}^2. \end{cases} \quad (46)$$

Additionally, though the Belle Collaboration has also announced measurements on  $R_K$  [27] and  $R_{K^*}$  [28] in several other bins, their results have comparatively larger uncertainties. The  $R_{K^{(*)}}$  ratios can constrain all the four new parameters.

### B. $b \rightarrow s\gamma$

The  $b \rightarrow s\gamma$  transition can occur at one-loop level as shown in Fig. 5, where the leptoquark and  $N_{\pm}$  were driving in the loop.

#### 1. $B \rightarrow X_s\gamma$

In the presence of NP, the branching ratio of the  $B \rightarrow X_s\gamma$  decay process induced by the  $b \rightarrow s\gamma$  transition is

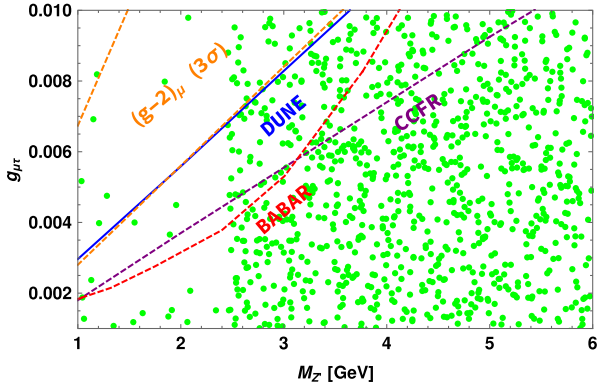


FIG. 6. Constraints on  $M'_Z - g_{\mu\tau}$  (left) and  $M_- - y_{qR}$  (right), obtained by using the branching ratios of  $b \rightarrow sll$ ,  $b \rightarrow s\gamma$  processes and the  $R_{K^{(*)}}$  parameters. Lines in the left panel denote the  $3\sigma$  consistent region of muon  $g - 2$  [150], exclusion limit from BABAR [121], and neutrino trident bounds from CCFR [124,125] and DUNE [66].

where

$$C_7^{\text{NP}} = -\frac{\sqrt{2}/3}{8G_F V_{tb} V_{ts}^* M_{S_1}^2} \frac{y_{qR}^2}{M_{S_1}^2} (J_1(\chi_-) \cos^2 \alpha + J_1(\chi_+) \sin^2 \alpha), \quad (48)$$

with the loop functions  $J_1(\chi_{\pm})$  [58]

$$J_1(\chi_{\pm}) = \frac{1 - 6\chi_{\pm} + 3\chi_{\pm}^2 + 2\chi_{\pm}^3 - 6\chi_{\pm}^2 \log \chi_{\pm}}{12(1 - \chi_{\pm})^4}. \quad (49)$$

The predicted SM branching ratio of the  $B \rightarrow X_s\gamma$  process [148]

$$\text{Br}(B \rightarrow X_s\gamma)|_{E_\gamma > 1.6 \text{ GeV}}^{\text{SM}} = (3.36 \pm 0.23) \times 10^{-4} \quad (50)$$

in relation with the corresponding experimental limit [149]

$$\text{Br}(B \rightarrow X_s\gamma)|_{E_\gamma > 1.6 \text{ GeV}}^{\text{Expt}} = (3.32 \pm 0.16) \times 10^{-4} \quad (51)$$

will impose constraint on the  $y_{qR}, M_-$  parameters.

Because of the absence of a  $Z'\mu\tau$  coupling in this model, the lepton flavor violating processes like  $B \rightarrow K^{(*)}\mu\tau$ ,  $\tau \rightarrow \mu\gamma$ , and  $\tau \rightarrow 3\mu$  are not allowed, thus we could not put a bound on new parameters. Using  $\text{Br}(B \rightarrow K^{(*)}ll)$  and  $R_{K^{(*)}}$  observables, we show the  $g_{\mu\tau}, M_{Z'}$  allowed parameters space in the left panel of Fig. 6. The region consistent with muon anomalous magnetic moment data is fully factored out by the constraint from the neutrino trident production. The validity of the effective field theory description in the present model lies above the electroweak scale i.e., in the range  $\sim(300-3000)$  GeV. It is indeed the favorable region of the ratio  $M_{Z'}/2g_{\mu\tau}$  and the lower value of this ratio is found to be

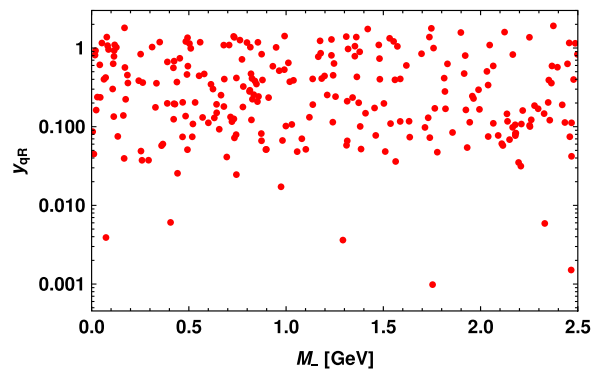


TABLE IV. The allowed regions of  $y_{qR}$ ,  $g_{\mu\tau}$ ,  $M_-$ , and  $M_{Z'}$  parameters.

Parameters	$y_{qR}$	$g_{\mu\tau}$	$M_-$ (GeV)	$M_{Z'}$ (GeV)
Allowed range	0–2.0	0–0.01	0–2.5	1–6

excluded by various experimental searches, as projected in the plot. The  $y_{qR}$ ,  $M_-$  allowed region consistent with the  $\text{Br}(B \rightarrow K^{(*)} ll)$ ,  $\text{Br}(B \rightarrow X_s \gamma)$ , and  $R_{K^{(*)}}$  observables is presented in the right panel of Fig. 6. The allowed range of all four new parameters consistent with flavor phenomenology is given in Table IV.

## VII. FOOTPRINTS ON $b \rightarrow s + \bar{E}$ DECAY MODES

The SM treats neutrinos as the only carrier of missing energy in  $b \rightarrow s$  transitions, i.e., the  $b \rightarrow s +$  missing energy can be described by the  $b \rightarrow s\nu\bar{\nu}$  decay modes in the SM. Here we consider the lepton flavor conserving  $b \rightarrow s\nu_l\bar{\nu}_l$  processes. In the SM, the general effective Hamiltonian responsible for the  $b \rightarrow s\nu_l\bar{\nu}_l$  transition is given by [37]

$$\mathcal{H}_{\text{eff}} = \frac{-4G_F}{\sqrt{2}} V_{tb} V_{ts}^* (C_L^\nu \mathcal{O}_L^\nu + C_R^\nu \mathcal{O}_R^\nu) + \text{H.c.}, \quad (52)$$

where

$$\begin{aligned} \mathcal{O}_L^\nu &= \frac{\alpha_{\text{em}}}{4\pi} (\bar{s}_R \gamma_\mu b_L) (\bar{\nu} \gamma^\mu (1 - \gamma_5) \nu), \\ \mathcal{O}_R^\nu &= \frac{\alpha_{\text{em}}}{4\pi} (\bar{s}_L \gamma_\mu b_R) (\bar{\nu} \gamma^\mu (1 - \gamma_5) \nu) \end{aligned} \quad (53)$$

are the dimension-six current-current operators with

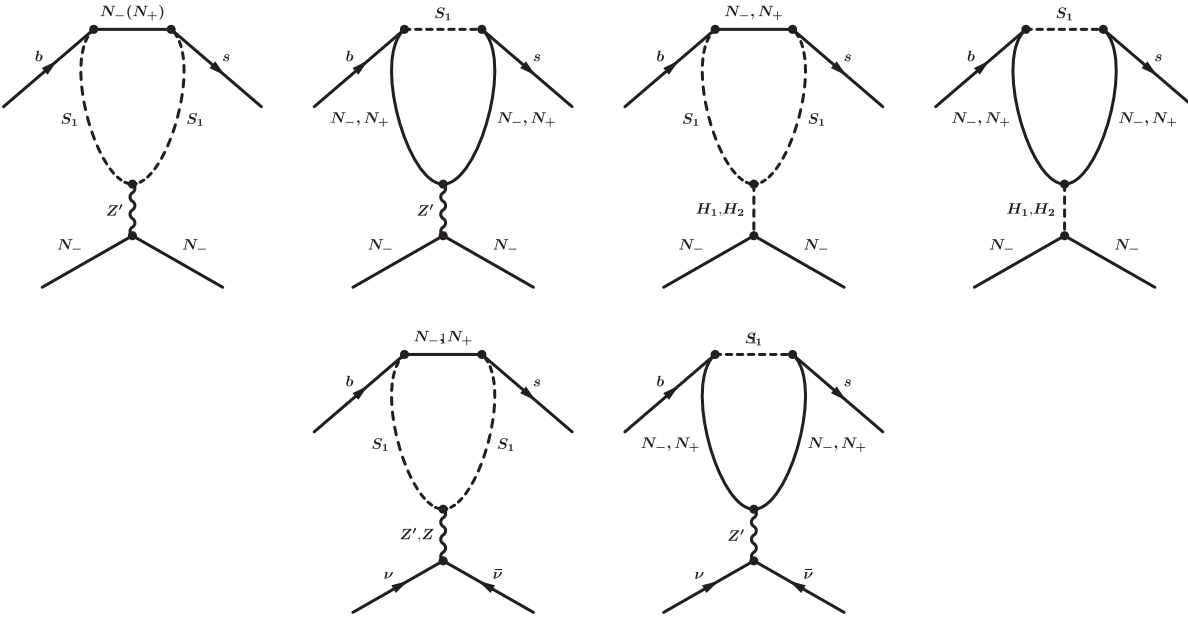


FIG. 7. One-loop penguin diagrams that provide nonzero contribution for  $b \rightarrow s +$  missing energy decay modes.

$$C_L^\nu = -X(x_t)/\sin^2\theta_w, \quad X(x_t) = X_0(x_t) + \frac{\alpha_s}{4\pi} X_1(x_t) \quad (54)$$

being the SM Wilson coefficient. The expressions for  $X_{0,1}(x_t)$  loop functions can be found in Refs. [151,152]. In the SM, the  $C_R^\nu$  Wilson coefficient is absent but can be generated in some new physics models.

In our model, all possible diagrams contributing to  $b \rightarrow s + \bar{E}$  processes are shown in Fig. 7. The first, third, fourth, and fifth diagrams in Fig. 7 will be suppressed by the factor  $m_q M_\pm/M_{S_1}^2$ . In the sixth diagram, the contributions of muon-neutrino and tau-neutrino cancel with each other in the leading order of NP due to their equal and opposite  $L_\mu - L_\tau$  charge. Thus, only the  $Z'$  exchanging second diagram will contribute to  $b \rightarrow s + \bar{E}$  processes in addition to the SM  $b \rightarrow s\nu_l\bar{\nu}_l$  modes.

### A. $B \rightarrow K + \bar{E}$

The total branching ratio of  $B \rightarrow K + \bar{E}$  decay is the sum of the branching ratio of semileptonic  $B \rightarrow K$  decay with a SM neutrino in the final state and the branching ratio of  $B \rightarrow KN_-N_-$  decay, i.e.,

$$\text{Br}(B \rightarrow K + \bar{E}) = \text{Br}(B \rightarrow K\nu\bar{\nu}) + \text{Br}(B \rightarrow KN_-N_-). \quad (55)$$

The branching ratio of the  $B \rightarrow K\nu_l\bar{\nu}_l$  decay process in the SM is given by [37]

$$\frac{d\text{Br}}{ds_B} = \tau_B \frac{G_F^2 \alpha^2}{256\pi^5} |V_{ts}^* V_{tb}|^2 M_B^5 \lambda^{3/2} (s_B, \tilde{M}_K^2, 1) |f_+^K(s_B)|^2 |C_L^\nu|^2, \quad (56)$$

where  $\tilde{M}_K = M_K/M_B$ ,  $s_B = s/M_B^2$ . The predicted branching ratio values of  $B^{+(0)} \rightarrow K^{+(0)}\nu_l\bar{\nu}_l$  by using input values from [7] and the corresponding experimental limits are tabulated in Table V.

The transition amplitude of the  $B \rightarrow KN_N$  process from the  $Z'$  exchanging one-loop penguin diagram is

$$\begin{aligned}\mathcal{M} &= \frac{1}{2^5\pi^2} \frac{y_{bR}^2 g_{\mu\tau}^2}{q^2 - M_{Z'}^2} \mathcal{V}_{sb}(\chi_-, \chi_+) [\bar{u}(p_B)\gamma^\mu(1 + \gamma_5)u(p_K)][\bar{v}(p_2)\gamma_\mu u(p_1)], \\ &= C^{\text{NP}}(q^2)[\bar{u}(p_B)\gamma^\mu(1 + \gamma_5)u(p_K)][\bar{v}(p_2)\gamma_\mu u(p_1)]\end{aligned}\quad (57)$$

where

$$C^{\text{NP}}(q^2) = \frac{1}{2^5\pi^2} \frac{y_{qR}^2 g_{\mu\tau}^2 \cos 2\beta \cos \alpha \sec \chi}{q^2 - M_{Z'}^2} \mathcal{V}_{sb}(\chi_-, \chi_+), \quad (58)$$

and  $p_B(p_K)$  is the four momenta of the  $B(K)$  meson and  $p_{1,2}$  are the momenta of the  $N_-$  fermion.

Using (57), the branching ratio of the  $B \rightarrow KN_N$  decay mode is given by

$$\frac{d\text{Br}}{dq^2} = \tau_B \frac{1}{2^7\pi^3 M_B^3} \sqrt{\lambda(M_B^2, M_K^2, q^2)} \beta_N f_+^2 \left( a_l(q^2) + \frac{c_l(q^2)}{3} \right), \quad (59)$$

where

$$\begin{aligned}a_l(q^2) &= q^2 |F_P|^2 + \left( \frac{\lambda(M_B^2, M_K^2, q^2)}{4} + 4M_-^2 M_B^2 \right) |F_A|^2 \\ &\quad + 2M_-(M_B^2 - M_K^2 + q^2) \text{Re}(F_P F_A^*), \\ c_l(q^2) &= -\frac{\lambda(M_B^2, M_K^2, q^2)}{4} \beta_N^2 |F_A|^2,\end{aligned}\quad (60)$$

with

$$\begin{aligned}F_A &= C^{\text{NP}}(q^2), \\ F_P &= M_- C^{\text{NP}}(q^2) \left[ \frac{M_B^2 - M_K^2}{q^2} \left( \frac{f_0(q^2)}{f_+(q^2)} - 1 \right) - 1 \right], \\ \beta_N &= \sqrt{1 - 4M_-^2/q^2}.\end{aligned}\quad (61)$$

TABLE V. The predicted branching ratios of  $B^{+(0)} \rightarrow M^{+(0)}\nu_l\bar{\nu}_l$  decays in the SM, where  $M = K^{(*)}, \phi$ . Their corresponding experimental limits are also noted in this table.

Decay process	Branching ratio in the SM	Experimental limit [7]
$B^0 \rightarrow K^0\nu_l\bar{\nu}_l$	$(4.53 \pm 0.267) \times 10^{-6}$	$< 2.6 \times 10^{-5}$
$B^+ \rightarrow K^+\nu_l\bar{\nu}_l$	$(4.9 \pm 0.288) \times 10^{-6}$	$< 1.6 \times 10^{-5}$
$B^0 \rightarrow K^{*0}\nu_l\bar{\nu}_l$	$(9.48 \pm 0.752) \times 10^{-6}$	$< 1.8 \times 10^{-5}$
$B^+ \rightarrow K^{*+}\nu_l\bar{\nu}_l$	$(1.03 \pm 0.06) \times 10^{-5}$	$< 4.0 \times 10^{-5}$
$B_s \rightarrow \phi\nu_l\bar{\nu}_l$	$(1.2 \pm 0.07) \times 10^{-5}$	$< 5.4 \times 10^{-5}$

### 1. $B \rightarrow K^* N_- N_-$

Similarly, the branching ratio of  $B \rightarrow K^* + E$  is given by

$$\text{Br}(B \rightarrow K^* + E) = \text{Br}(B \rightarrow K^*\nu_l\bar{\nu}) + \text{Br}(B \rightarrow K^*N_-N_-). \quad (62)$$

The decay rate of the  $B \rightarrow K^*\nu_l\bar{\nu}$  decay mode in terms of  $s_B$  and  $\cos \theta$  is given as [37,153]

$$\frac{d^2\Gamma}{ds_B d\cos \theta} = \frac{3}{4} \frac{d\Gamma_T}{ds_B} \sin^2 \theta + \frac{3}{2} \frac{d\Gamma_L}{ds_B} \cos^2 \theta, \quad (63)$$

where the longitudinal and transverse polarization decay rates are

$$\frac{d\Gamma_L}{ds_B} = 3M_B^2 |A_0|^2, \quad \frac{d\Gamma_T}{ds_B} = 3M_B^2 (|A_\perp|^2 + |A_\parallel|^2), \quad (64)$$

with the transversity amplitudes  $A_{\perp,\parallel,0}$  in terms of form factor and Wilson coefficients are defined as

$$\begin{aligned}A_\perp(s_B) &= 2N\sqrt{2}\lambda^{1/2}(1, \tilde{M}_{K^*}^2, s_B) C_L^\nu \frac{V(s_B)}{(1 + \tilde{M}_{K^*})}, \\ A_\parallel(s_B) &= -2N\sqrt{2}(1 + \tilde{M}_{K^*}) C_L^\nu A_1(s_B), \\ A_0(s_B) &= -\frac{NC_L^\nu}{\tilde{M}_{K^*}\sqrt{s_B}} \left[ (1 - \tilde{M}_{K^*}^2 - s_B)(1 + \tilde{M}_{K^*}) A_1(s_B) \right. \\ &\quad \left. - \lambda(1, \tilde{M}_{K^*}^2, s_B) \frac{A_2(s_B)}{1 + \tilde{M}_{K^*}} \right],\end{aligned}\quad (65)$$

where  $\tilde{M}_{K^*} = M_{K^*}/M_B$  and

$$N = V_{tb} V_{ts}^* \left[ \frac{G_F^2 \alpha^2 M_B^3}{3 \cdot 2^{10} \pi^5} s_B \lambda^{1/2}(1, \tilde{M}_{K^*}^2, s_B) \right]^{1/2}. \quad (66)$$

The same expression can be used for  $B_s \rightarrow \phi\nu_l\bar{\nu}_l$ . Now using all the required input values from [7], the  $B_{(s)} \rightarrow K^*(\phi)$  form factor from [147], the branching ratio of  $B_{(s)} \rightarrow K^*(\phi)\nu_l\bar{\nu}_l$ , and their corresponding experimental limits are presented in Table V.

TABLE VI. Benchmark values of  $y_{qR}$ ,  $M_-$ ,  $g_{\mu\tau}$ , and  $M_{Z'}$  parameters used in our analysis.

Benchmark	$y_{qR}$	$g_{\mu\tau}$	$M_-$ (GeV)	$M_{Z'}$ (GeV)
Benchmark-I	2.0	0.002	1.7	4
Benchmark-II	2.0	0.008	1.8	4.8

The decay rate of the  $B \rightarrow K^* N_- N_-$  process is given by

$$\frac{d\Gamma}{dq^2} = \frac{3}{4} \left( J_1 - \frac{J_2}{3} \right), \quad J_{1,2} = 2J_{1,2}^s + J_{1,2}^c, \quad (67)$$

where

$$\begin{aligned} J_1^s &= \frac{(2 + \beta_N^2)}{4} [|A_\perp^L|^2 + |A_\parallel^L|^2 + (L \rightarrow R)] \\ &\quad + \frac{4m_N^2}{q^2} \text{Re}(A_\perp^L A_\perp^{R*} + A_\parallel^L A_\parallel^{R*}), \\ J_1^c &= |A_0^L|^2 + |A_0^R|^2 + \frac{4M_-^2}{q^2} [|A_t|^2 + 2\text{Re}(A_0^L A_0^{R*})], \\ J_2^s &= \frac{\beta_I^2}{4} [|A_\perp^L|^2 + |A_\parallel^L|^2 + (L \rightarrow R)], \\ J_2^c &= -\beta_I^2 [|A_0^L|^2 + (L \rightarrow R)], \end{aligned} \quad (68)$$

where the transversity amplitudes in terms of the form factors and new functions are given as

$$\begin{aligned} A_{\perp L,R} &= \mp N_2 C^{\text{NP}}(q^2) \sqrt{2\lambda(M_{K^*}^2, M_B^2, q^2)} \frac{V(q^2)}{M_B + M_{K^*}}, \\ A_{\parallel L,R} &= \pm N_2 C^{\text{NP}}(q^2) \sqrt{2(M_B^2 - M_{K^*}^2)} \frac{A_1(q^2)}{M_B - M_{K^*}}, \\ A_{0L,R} &= \pm \frac{N_2 C^{\text{NP}}(q^2)}{2M_{K^*}\sqrt{s}} \left( (M_B^2 - M_{K^*}^2 - q^2)(M_B + M_{K^*})A_1(q^2) - \lambda(M_{K^*}^2, M_B^2, q^2) \frac{A_2(q^2)}{M_B + M_{K^*}} \right), \\ A_t &= 2N_2 C^{\text{NP}}(q^2) \sqrt{\frac{\lambda(M_{K^*}^2, M_B^2, q^2)}{q^2}} A_0(q^2), \end{aligned} \quad (69)$$

and

$$N_2 = \left[ \frac{1}{3 \cdot 2^9 \pi^3 M_B^3} q^2 \beta_N \sqrt{\lambda(M_{K^*}^2, M_B^2, q^2)} \right]^{1/2}. \quad (70)$$

For numerical estimation, we took the required input parameters like mass of particles, lifetime of  $B_{(s)}$  meson, and CKM parameters from [7], and the  $B_{(s)} \rightarrow K^*(\phi)$  form factors from [147]. We have taken two different benchmark values of all four new parameters, which are allowed by both the DM and flavor phenomenology, as presented in Table VI.

By using all the discussed input parameters, we show the branching ratios of  $B^0 \rightarrow K^0 N_- N_-$  (top panel),  $B^0 \rightarrow K^{*0} N_- N_-$  (middle panel), and  $B_s \rightarrow \phi N_- N_-$  (bottom panel) with respect to  $q^2$  in Fig. 8. Here, the left panel figures are obtained by using the benchmark-I values and the right panel plots are for benchmark-II values. The estimated numerical values of the branching ratios of  $b \rightarrow s N_- N_-$  processes for both sets of benchmark values are tabulated in Table VII. For benchmark-I, there is a singularity at  $q^2 = M_{Z'}^2$ , i.e.,  $q^2 = 16 \text{ GeV}^2$ . In order to avoid the singularity, we put the cuts at  $(M_{Z'} - 0.002)^2 \leq q^2 \leq (M_{Z'} + 0.002)^2 \text{ GeV}^2$ . In Table VIII, we present the branching ratios of  $b \rightarrow s E$  which are the sum of the branching ratios of  $b \rightarrow s\nu_l\bar{\nu}_l$  and  $b \rightarrow sN_-N_-$  decay processes. We observe that the addition

of the  $b \rightarrow s N_- N_-$  process provides deviation from the SM predictions and is within the experimental limits.

## VIII. CONCLUSION

In this work, we have investigated light GeV scale dark matter and flavor anomalies in a simple  $U(1)_{L_\mu - L_\tau}$  variant with heavy neutral fermions and a  $(\bar{3}, 1, 1/3)$  scalar leptoquark. The  $U(1)$  associated gauge boson ( $Z'$ ) plays a key role and is explored in the low mass regime. The lightest fermion is a stable dark matter and the resonance in  $Z'$  portal annihilation channels brings down the relic density to meet Planck data. A WIMP-nucleon cross section of spin-dependent type is obtained in a leptoquark portal and is looked up for consistency with CDMSlite bound. A benchmark is provided for generating light neutrino mass radiatively with small Yukawa.

We have constrained the new parameters by using the branching ratios of  $b \rightarrow sll$ ,  $b \rightarrow sy$ , and the  $R_{K^{(*)}}$  observables. We have taken two different sets of benchmark values of new parameters (which are compatible with both the dark matter and flavor phenomenology) and have shown the impact on rare  $B$  meson decays to missing energy. There exist only experimental upper limits on the branching ratios of  $b \rightarrow s + \text{missing energy}$  processes. In the SM, the missing energy can be carried away by a pair of neutrino, i.e., by  $b \rightarrow s\nu_l\bar{\nu}_l$  processes. We have assumed the missing energy part as a pair of dark matter in the proposed

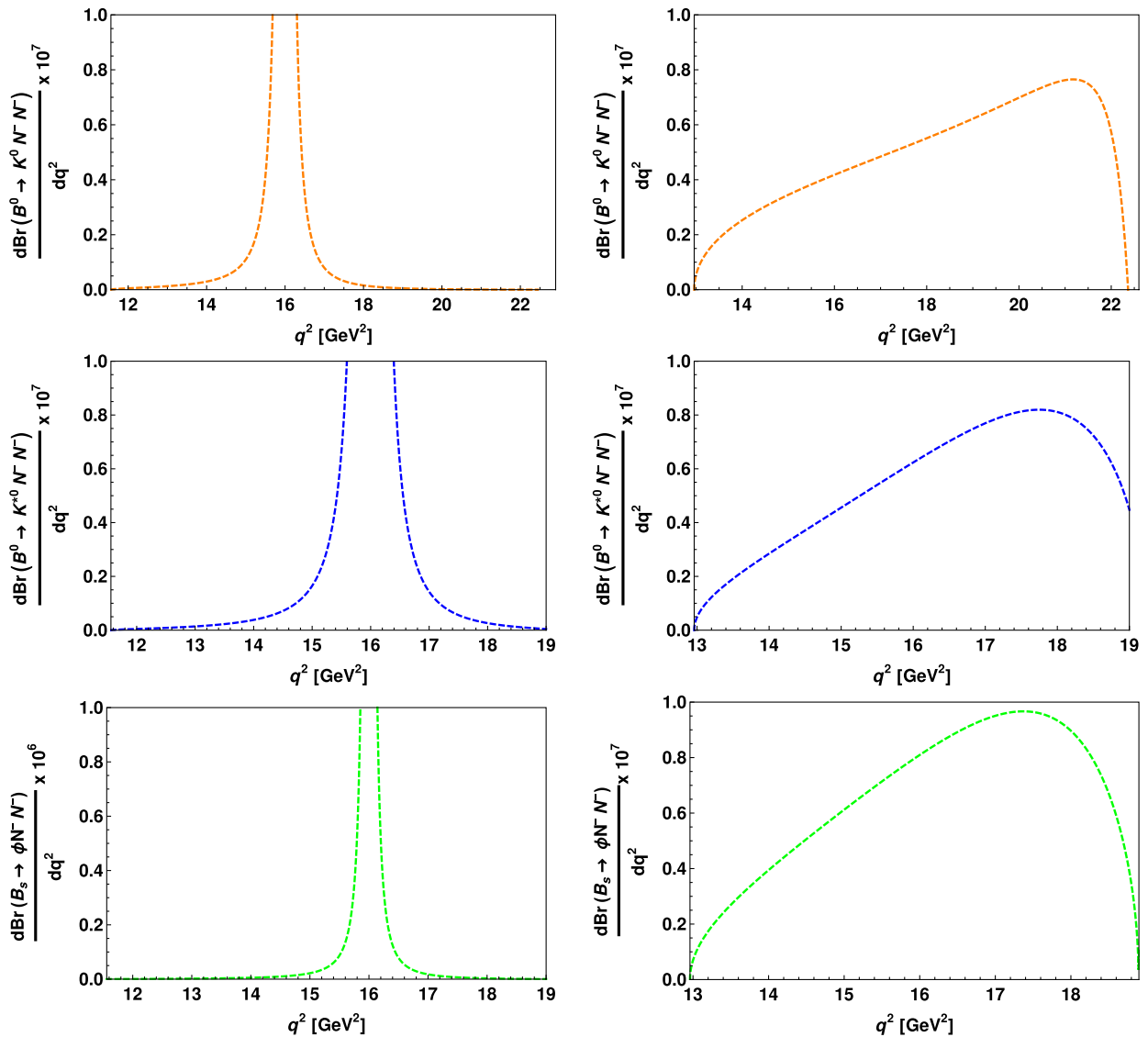


FIG. 8. The branching ratios of  $B^0 \rightarrow K^0 N_- N_-$  (left, top),  $B^0 \rightarrow K^{*0} N_- N_-$  (left, middle), and  $B_s \rightarrow \phi N_- N_-$  (left, bottom) with respect to  $q^2$  for benchmark-I. The corresponding plots obtained by using benchmark-II are presented in the right panel.

TABLE VII. The predicted branching ratios of  $b \rightarrow s N_- N_-$  processes for two different benchmark values of new parameters, which are compatible with both the dark matter and the flavor sectors.

$\text{Br}(b \rightarrow s N_- N_-)$	Values using benchmark-I	Values using benchmark-II
$\text{Br}(B^0 \rightarrow K^0 N_- N_-)$	$1.92 \times 10^{-6}$	$4.1 \times 10^{-7}$
$\text{Br}(B^+ \rightarrow K^+ N_- N_-)$	$2.072 \times 10^{-6}$	$2.6 \times 10^{-7}$
$\text{Br}(B^0 \rightarrow K^{*0} N_- N_-)$	$3.23 \times 10^{-6}$	$3.3 \times 10^{-7}$
$\text{Br}(B^+ \rightarrow K^{*+} N_- N_-)$	$3.51 \times 10^{-6}$	$3.61 \times 10^{-7}$
$\text{Br}(B_s \rightarrow \phi N_- N_-)$	$4.18 \times 10^{-6}$	$3.93 \times 10^{-7}$

TABLE VIII. The predicted branching ratios of  $b \rightarrow s\bar{E}$  processes for two different benchmark values of new parameters.

$\text{Br}(b \rightarrow s\bar{E})$	Benchmark-I	Benchmark-II	Experimental Limit [7]
$\text{Br}(B^0 \rightarrow K^0\bar{E})$	$0.645 \times 10^{-5}$	$0.457 \times 10^{-5}$	$< 2.6 \times 10^{-5}$
$\text{Br}(B^+ \rightarrow K^+\bar{E})$	$0.697 \times 10^{-5}$	$0.516 \times 10^{-5}$	$< 1.6 \times 10^{-5}$
$\text{Br}(B^0 \rightarrow K^{*0}\bar{E})$	$1.271 \times 10^{-5}$	$0.981 \times 10^{-5}$	$< 1.8 \times 10^{-5}$
$\text{Br}(B^+ \rightarrow K^{*+}\bar{E})$	$1.381 \times 10^{-5}$	$1.066 \times 10^{-5}$	$< 4.0 \times 10^{-5}$
$\text{Br}(B_s \rightarrow \phi\bar{E})$	$1.618 \times 10^{-5}$	$1.24 \times 10^{-5}$	$< 5.4 \times 10^{-3}$

$L_\mu - L_\tau$  scenario. We have shown our prediction for the branching ratios of  $b \rightarrow s\bar{E}$  for two sets of benchmark values which are within the experimental limits. The observation of these modes at LHCb and Belle-II experiments would provide strong hints for the existence of light fermionic dark matter.

### ACKNOWLEDGMENTS

S. S. and R. M. would like to thank the University of Hyderabad for financial support through the IoE project Grant No. IoE/RC1/RC1-20-012. R. M. acknowledges the support from SERB, Government of India through Grant No. EMR/2017/001448.

### APPENDIX A: RELEVANT VERTICES AND COUPLINGS

The fermion-gauge vertices and fermion-scalar vertices along with the corresponding couplings are provided in Tables IX and X respectively.

TABLE IX. Fermion-gauge vertices and couplings.

Vertex	Coupling
$\bar{\mu}\gamma^\mu(c_V^\mu - c_A^\mu\gamma^5)\mu Z_\mu$	$\frac{g}{2\cos\theta_w}(\cos\alpha - \sin\alpha\sin\theta_w\tan\chi)$
$\bar{\tau}\gamma^\mu(c_V^\tau - c_A^\tau\gamma^5)\tau Z_\mu$	$\frac{g}{2\cos\theta_w}(\cos\alpha - \sin\alpha\sin\theta_w\tan\chi)$
$\bar{\nu}_\mu\gamma^\mu(c_V^{\nu_\mu} - c_A^{\nu_\mu}\gamma^5)\nu_\mu Z_\mu$	$\frac{g}{2\cos\theta_w}(\cos\alpha - \sin\alpha\sin\theta_w\tan\chi)$
$\bar{\nu}_\tau\gamma^\mu(c_V^{\nu_\tau} - c_A^{\nu_\tau}\gamma^5)\nu_\tau Z_\mu$	$\frac{g}{2\cos\theta_w}(\cos\alpha - \sin\alpha\sin\theta_w\tan\chi)$
$\bar{N}_-\gamma^\mu\gamma^5 N_- Z_\mu$	$g_{\mu\tau}\cos 2\beta \sin\alpha \sec\chi$
$\bar{N}_+\gamma^\mu\gamma^5 N_+ Z_\mu$	$-g_{\mu\tau}\cos 2\beta \sin\alpha \sec\chi$
$(\bar{N}_-\gamma^\mu\gamma^5 N_+ + \bar{N}_+\gamma^\mu\gamma^5 N_-)Z_\mu$	$g_{\mu\tau}\sin 2\beta \sin\alpha \sec\chi$
$(S_1\partial^\mu S_1^\dagger - S_1^\dagger\partial^\mu S_1)Z_\mu$	$\frac{g'}{3}(-\cos\alpha\sin\theta_w + \sin\alpha\tan\chi) + g_{\mu\tau}\sin\alpha\sec\chi$
$\bar{\mu}\gamma^\mu\mu A_\mu$	$g\sin\theta_w$
$\bar{\tau}\gamma^\mu\tau A_\mu$	$g\sin\theta_w$
$(S_1\partial^\mu S_1^\dagger - S_1^\dagger\partial^\mu S_1)A_\mu$	$\frac{g'}{3}\cos\theta_w$
$\bar{\mu}\gamma^\mu\mu Z'_\mu$	$g_{\mu\tau}\cos\alpha\sec\chi$
$\bar{\tau}\gamma^\mu\tau Z'_\mu$	$-g_{\mu\tau}\cos\alpha\sec\chi$
$\bar{\nu}_\mu\gamma^\mu(1 - \gamma^5)\nu_\mu Z'_\mu$	$g_{\mu\tau}\cos\alpha\sec\chi$
$\bar{\nu}_\tau\gamma^\mu(1 - \gamma^5)\nu_\tau Z'_\mu$	$-g_{\mu\tau}\cos\alpha\sec\chi$
$\bar{N}_-\gamma^\mu\gamma^5 N_- Z'_\mu$	$-g_{\mu\tau}\cos 2\beta \cos\alpha \sec\chi$
$\bar{N}_+\gamma^\mu\gamma^5 N_+ Z'_\mu$	$g_{\mu\tau}\cos 2\beta \cos\alpha \sec\chi$
$(\bar{N}_-\gamma^\mu\gamma^5 N_+ + \bar{N}_+\gamma^\mu\gamma^5 N_-)Z'_\mu$	$-g_{\mu\tau}\sin 2\beta \cos\alpha \sec\chi$
$(S_1\partial^\mu S_1^\dagger - S_1^\dagger\partial^\mu S_1)Z'_\mu$	$-\frac{g'}{3}(\sin\alpha\sin\theta_w + \cos\alpha\tan\chi) - g_{\mu\tau}\cos\alpha\sec\chi$

### APPENDIX B: LOOP FUNCTIONS

The  $b \rightarrow sll$  loop function, used in Sec. VI is given by

$$\begin{aligned} \mathcal{V}_{sb}(\chi_-, \chi_+) = & \sin^2 2\beta \cos\alpha \sec\chi (1 + 4\sqrt{\chi_-\chi_+}j(\chi_-, \chi_+)) \\ & - 2k(\chi_-, \chi_+) + 2(\sin^2\beta I(\chi_+) \\ & + \cos^2\beta I(\chi_-)) \cos^2\beta \cos\alpha \sec\chi, \end{aligned} \quad (\text{B1})$$

where

$$\begin{aligned} f(\chi_1, \chi_2, \chi_3, \dots) \equiv & \frac{f(\chi_1, \chi_3, \dots) - f(\chi_2, \chi_3, \dots)}{\chi_1 - \chi_2}, \\ f = j, \kappa, \end{aligned} \quad (\text{B2})$$

with

$$j(\chi) = \frac{\chi \log \chi}{\chi - 1}, \quad (\text{B3})$$

TABLE X. Fermion-scalar vertices and couplings.

Vertex	Coupling
$\bar{\mu}H_1$	$\frac{m_\mu}{v} \cos \zeta$
$\bar{\tau}H_1$	$\frac{m_\tau}{v} \cos \zeta$
$\bar{N}_-^c N_- H_1$	$-\frac{1}{\sqrt{2}}(f_\mu \cos^2 \beta + f_\tau \sin^2 \beta) \sin \zeta$
$\bar{N}_+^c N_+ H_1$	$-\frac{1}{\sqrt{2}}(f_\mu \sin^2 \beta + f_\tau \cos^2 \beta) \sin \zeta$
$\bar{N}_-^c N_+ H_1$	$-\frac{1}{\sqrt{2}}(f_\mu - f_\tau) \sin 2\beta \sin \zeta$
$S_1^\dagger S_1 H_1$	$\lambda_{HS} v \cos \zeta - \lambda_{S\phi} v_2 \sin \zeta$
$\bar{\mu}H_2$	$\frac{m_\mu}{v} \sin \zeta$
$\bar{\tau}H_2$	$\frac{m_\tau}{v} \sin \zeta$
$\bar{N}_-^c N_- H_2$	$\frac{1}{\sqrt{2}}(f_\mu \cos^2 \beta + f_\tau \sin^2 \beta) \cos \zeta$
$\bar{N}_+^c N_+ H_2$	$\frac{1}{\sqrt{2}}(f_\mu \sin^2 \beta + f_\tau \cos^2 \beta) \cos \zeta$
$\bar{N}_-^c N_+ H_2$	$\frac{1}{\sqrt{2}}(f_\mu - f_\tau) \sin 2\beta \cos \zeta$
$S_1^\dagger S_1 H_2$	$\lambda_{HS} v \sin \zeta + \lambda_{S\phi} v_2 \cos \zeta$
$\bar{d}_{qR}^c S_1 N_- + \text{h.c.}$	$y_{qR} \cos \beta$
$\bar{d}_{qR}^c S_1 N_+ + \text{h.c.}$	$y_{qR} \sin \beta$

$$\kappa(\chi) = \frac{\chi^2 \log \chi}{\chi - 1}, \quad (\text{B4})$$

$$I(\chi) = \frac{-3\chi^2 + 4\chi - 1 + 2\chi^2 \log \chi}{8(\chi - 1)^2}. \quad (\text{B5})$$

### APPENDIX C: EFFECTIVE WILSON COEFFICIENTS

The effective  $C_7^{\text{eff}}$  and  $C_9^{\text{eff}}$  Wilson coefficients including the four-quark and gluon dipole operators, as mentioned in Eq. (25) are given as [141]

$$C_7^{\text{eff}} = C_7 - \frac{1}{3} \left[ C_3 + \frac{4}{3} C_4 + 20C_5 + \frac{80}{3} C_6 \right] + \frac{\alpha_s}{4\pi} [(C_1 - 6C_2)A(q^2) - C_8 F_8^{(7)}(q^2)], \quad (\text{C1})$$

$$C_9^{\text{eff}} = C_9 + h(0, q^2) \left[ \frac{4}{3} C_1 + C_2 + \frac{11}{2} C_3 - \frac{2}{3} C_4 + 52C_5 - \frac{32}{3} C_6 \right] - \frac{1}{2} h(m_b, q^2) \left[ 7C_3 + \frac{4}{3} C_4 + 76C_5 + \frac{64}{3} C_6 \right] + \frac{4}{3} \left[ C_3 + \frac{16}{3} C_5 + \frac{16}{9} C_6 \right] + \frac{\alpha_s}{4\pi} [C_1(B(q^2) + 4C(q^2)) - 3C_2(2B(q^2) - C(q^2)) - C_8 F_8^{(9)}(q^2)] + 8 \frac{m_c^2}{q^2} \left[ \left( \frac{4}{9} C_1 + \frac{1}{3} C_2 \right) (1 + \lambda_u) + 2C_3 + 20C_5 \right], \quad (\text{C2})$$

where  $\lambda_u = (V_{ub} V_{us}^*) / (V_{tb} V_{ts}^*)$  and the functions  $h(m_i, q^2)$  and  $A, B, C, F_8^{(7,9)}$  can be found in Refs. [142,143].

- 
- [1] F. Zwicky, *Astrophys. J.* **86**, 217 (1937).
  - [2] V. C. Rubin and W. K. Ford, Jr., *Astrophys. J.* **159**, 379 (1970).
  - [3] D. Clowe, A. Gonzalez, and M. Markevitch, *Astrophys. J.* **604**, 596 (2004).
  - [4] G. Bertone, D. Hooper, and J. Silk, *Phys. Rep.* **405**, 279 (2005).
  - [5] N. Arkani-Hamed, D. P. Finkbeiner, T. R. Slatyer, and N. Weiner, *Phys. Rev. D* **79**, 015014 (2009).
  - [6] S. Dodelson and L. M. Widrow, *Phys. Rev. Lett.* **72**, 17 (1994).
  - [7] P. A. Zyla *et al.* (Particle Data Group), *Prog. Theor. Exp. Phys.* **2020**, 083C01 (2020).
  - [8] A. Sakharov, *Sov. Phys. Usp.* **34**, 392 (1991).
  - [9] E. W. Kolb and S. Wolfram, *Nucl. Phys.* **B172**, 224 (1980); *Nucl. Phys.* **B195**, 542(E) (1982).
  - [10] S. Davidson, E. Nardi, and Y. Nir, *Phys. Rep.* **466**, 105 (2008).
  - [11] W. Buchmuller, P. Di Bari, and M. Plumacher, *Ann. Phys. (Amsterdam)* **315**, 305 (2005).
  - [12] H. Murayama, in *Les Houches Summer School - Session 86: Particle Physics and Cosmology: The Fabric of Spacetime* (2007) [[arXiv:0704.2276](#)].
  - [13] R. Aaij *et al.* (LHCb Collaboration), *Phys. Rev. Lett.* **113**, 151601 (2014).
  - [14] R. Aaij *et al.* (LHCb Collaboration), *Phys. Rev. Lett.* **122**, 191801 (2019).
  - [15] R. Aaij *et al.* (LHCb Collaboration), [arXiv:2103.11769](#).

- [16] C. Bobeth, G. Hiller, and G. Piranishvili, *J. High Energy Phys.* **12** (2007) 040.
- [17] M. Bordone, G. Isidori, and A. Patti, *Eur. Phys. J. C* **76**, 440 (2016).
- [18] R. Aaij *et al.* (LHCb Collaboration), *J. High Energy Phys.* **08** (2017) 055.
- [19] B. Capdevila, A. Crivellin, S. Descotes-Genon, J. Matias, and J. Virto, *J. High Energy Phys.* **01** (2018) 093.
- [20] Y. S. Amhis *et al.* (HFLAV Collaboration), *Eur. Phys. J. C* **81**, 226 (2021).
- [21] H. Na, C. M. Bouchard, G. P. Lepage, C. Monahan, and J. Shigemitsu (HPQCD Collaboration), *Phys. Rev. D* **92**, 054510 (2015); *Phys. Rev. D* **93**, 119906(E) (2016).
- [22] S. Fajfer, J. F. Kamenik, and I. Nisandzic, *Phys. Rev. D* **85**, 094025 (2012).
- [23] S. Fajfer, J. F. Kamenik, I. Nisandzic, and J. Zupan, *Phys. Rev. Lett.* **109**, 161801 (2012).
- [24] R. Aaij *et al.* (LHCb Collaboration), *Phys. Rev. Lett.* **120**, 121801 (2018).
- [25] W.-F. Wang, Y.-Y. Fan, and Z.-J. Xiao, *Chin. Phys. C* **37**, 093102 (2013).
- [26] M. A. Ivanov, J. G. Korner, and P. Santorelli, *Phys. Rev. D* **71**, 094006 (2005); *Phys. Rev. D* **75**, 019901(E) (2007).
- [27] S. Choudhury *et al.* (Belle Collaboration), *J. High Energy Phys.* **03** (2021) 105.
- [28] A. Abdesselam *et al.* (Belle Collaboration), *Phys. Rev. Lett.* **126**, 161801 (2021).
- [29] R. Aaij *et al.* (LHCb Collaboration), *Phys. Rev. Lett.* **111**, 191801 (2013).
- [30] R. Aaij *et al.* (LHCb Collaboration), *J. High Energy Phys.* **02** (2016) 104.
- [31] W. Adam *et al.* (ATLAS, Belle II, CMS, and LHCb Collaboration), Proceedings of the LHCSci2016 Workshop, arXiv:1607.01212.
- [32] R. Aaij *et al.* (LHCb Collaboration), *J. High Energy Phys.* **06** (2014) 133.
- [33] R. Aaij *et al.* (LHCb Collaboration), *J. High Energy Phys.* **07** (2013) 084.
- [34] A. Badin and A. A. Petrov, *Phys. Rev. D* **82**, 034005 (2010).
- [35] M. J. Aslam and C.-D. Lu, *Chin. Phys. C* **33**, 332 (2009).
- [36] T. M. Aliev, A. S. Cornell, and N. Gaur, *J. High Energy Phys.* **07** (2007) 072.
- [37] W. Altmannshofer, A. J. Buras, D. M. Straub, and M. Wick, *J. High Energy Phys.* **04** (2009) 022.
- [38] C. S. Kim and R.-M. Wang, *Phys. Rev. D* **77**, 094006 (2008).
- [39] J. H. Jeon, C. S. Kim, J. Lee, and C. Yu, *Phys. Lett. B* **636**, 270 (2006).
- [40] C. S. Kim and R.-M. Wang, *Phys. Lett. B* **681**, 44 (2009).
- [41] B. B. Sirvanli, *Mod. Phys. Lett. A* **23**, 347 (2008).
- [42] C. Smith, arXiv:1012.4398.
- [43] N. Mahajan, *Phys. Rev. D* **68**, 034012 (2003).
- [44] X.-G. He, G. C. Joshi, H. Lew, and R. R. Volkas, *Phys. Rev. D* **44**, 2118 (1991).
- [45] X. G. He, G. C. Joshi, H. Lew, and R. R. Volkas, *Phys. Rev. D* **43**, R22 (1991).
- [46] E. Ma, D. P. Roy, and S. Roy, *Phys. Lett. B* **525**, 101 (2002).
- [47] S. Baek and P. Ko, *J. Cosmol. Astropart. Phys.* **10** (2009) 011.
- [48] W. Altmannshofer, S. Gori, M. Pospelov, and I. Yavin, *Phys. Rev. D* **89**, 095033 (2014).
- [49] J. Heeck, M. Holthausen, W. Rodejohann, and Y. Shimizu, *Nucl. Phys. B* **896**, 281 (2015).
- [50] A. Crivellin, G. D'Ambrosio, and J. Heeck, *Phys. Rev. Lett.* **114**, 151801 (2015).
- [51] K. Fuyuto, W.-S. Hou, and M. Kohda, *Phys. Rev. D* **93**, 054021 (2016).
- [52] S. Patra, W. Rodejohann, and C. E. Yaguna, *J. High Energy Phys.* **09** (2016) 076.
- [53] A. Biswas, S. Choubey, and S. Khan, *J. High Energy Phys.* **09** (2016) 147.
- [54] W. Altmannshofer, S. Gori, S. Profumo, and F. S. Queiroz, *J. High Energy Phys.* **12** (2016) 106.
- [55] T. Araki, S. Hoshino, T. Ota, J. Sato, and T. Shimomura, *Phys. Rev. D* **95**, 055006 (2017).
- [56] C.-H. Chen and T. Nomura, *Phys. Rev. D* **96**, 095023 (2017).
- [57] C.-H. Chen and T. Nomura, *Phys. Lett. B* **777**, 420 (2018).
- [58] S. Baek, *Phys. Lett. B* **781**, 376 (2018).
- [59] M. Bauer, P. Foldenauer, and J. Jaeckel, *J. High Energy Phys.* **07** (2018) 094.
- [60] A. Kamada, K. Kaneta, K. Yanagi, and H.-B. Yu, *J. High Energy Phys.* **06** (2018) 117.
- [61] S. N. Gninenko and N. V. Krasnikov, *Phys. Lett. B* **783**, 24 (2018).
- [62] T. Nomura and H. Okada, *Phys. Rev. D* **97**, 095023 (2018).
- [63] H. Banerjee and S. Roy, *Phys. Rev. D* **99**, 035035 (2019).
- [64] J. Heeck, M. Lindner, W. Rodejohann, and S. Vogl, *SciPost Phys.* **6**, 038 (2019).
- [65] M. Escudero, D. Hooper, G. Krnjaic, and M. Pierre, *J. High Energy Phys.* **03** (2019) 071.
- [66] W. Altmannshofer, S. Gori, J. Martín-Albo, A. Sousa, and M. Wallbank, *Phys. Rev. D* **100**, 115029 (2019).
- [67] A. Biswas and A. Shaw, *J. High Energy Phys.* **05** (2019) 165.
- [68] K. Kowalska, D. Kumar, and E. M. Sessolo, *Eur. Phys. J. C* **79**, 840 (2019).
- [69] Z. Kang and Y. Shigekami, *J. High Energy Phys.* **11** (2019) 049.
- [70] A. S. Joshipura, N. Mahajan, and K. M. Patel, *J. High Energy Phys.* **03** (2020) 001.
- [71] Z.-L. Han, R. Ding, S.-J. Lin, and B. Zhu, *Eur. Phys. J. C* **79**, 1007 (2019).
- [72] Y. Jho, S. M. Lee, S. C. Park, Y. Park, and P.-Y. Tseng, *J. High Energy Phys.* **04** (2020) 086.
- [73] D. W. P. d. Amaral, D. G. Cerdeno, P. Foldenauer, and E. Reid, *J. High Energy Phys.* **12** (2020) 155.
- [74] D. Borah, S. Mahapatra, D. Nanda, and N. Sahu, *Phys. Lett. B* **811**, 135933 (2020).
- [75] G.-y. Huang, F. S. Queiroz, and W. Rodejohann, *Phys. Rev. D* **103**, 095005 (2021).
- [76] D. Borah, M. Dutta, S. Mahapatra, and N. Sahu, *Phys. Lett. B* **820**, 136577 (2021).
- [77] S. Singirala, S. Sahoo, and R. Mohanta, *Phys. Rev. D* **99**, 035042 (2019).

- [78] H. Georgi and S. L. Glashow, *Phys. Rev. Lett.* **32**, 438 (1974).
- [79] H. Fritzsch and P. Minkowski, *Ann. Phys. (N.Y.)* **93**, 193 (1975).
- [80] P. Langacker, *Phys. Rep.* **72**, 185 (1981).
- [81] H. Georgi, *AIP Conf. Proc.* **23**, 575 (1975).
- [82] J. C. Pati and A. Salam, *Phys. Rev. D* **10**, 275 (1974); *Phys. Rev. D* **11**, 703(E) (1975).
- [83] J. C. Pati and A. Salam, *Phys. Rev. D* **8**, 1240 (1973).
- [84] J. C. Pati and A. Salam, *Phys. Rev. Lett.* **31**, 661 (1973).
- [85] O. U. Shanker, *Nucl. Phys.* **B206**, 253 (1982).
- [86] O. U. Shanker, *Nucl. Phys.* **B204**, 375 (1982).
- [87] D. B. Kaplan, *Nucl. Phys.* **B365**, 259 (1991).
- [88] B. Schrempp and F. Schrempp, *Phys. Lett.* **153B**, 101 (1985).
- [89] B. Gripaios, *J. High Energy Phys.* **02** (2010) 045.
- [90] A. K. Alok, B. Bhattacharya, A. Datta, D. Kumar, J. Kumar, and D. London, *Phys. Rev. D* **96**, 095009 (2017).
- [91] D. Beirevi and O. Sumensari, *J. High Energy Phys.* **08** (2017) 104.
- [92] G. Hiller and I. Nisandzic, *Phys. Rev. D* **96**, 035003 (2017).
- [93] G. D'Amico, M. Nardecchia, P. Panci, F. Sannino, A. Strumia, R. Torre, and A. Urbano, *J. High Energy Phys.* **09** (2017) 010.
- [94] D. Beirevi, S. Fajfer, N. Konik, and O. Sumensari, *Phys. Rev. D* **94**, 115021 (2016).
- [95] M. Bauer and M. Neubert, *Phys. Rev. Lett.* **116**, 141802 (2016).
- [96] L. Calibbi, A. Crivellin, and T. Ota, *Phys. Rev. Lett.* **115**, 181801 (2015).
- [97] M. Freytsis, Z. Ligeti, and J. T. Ruderman, *Phys. Rev. D* **92**, 054018 (2015).
- [98] B. Dumont, K. Nishiwaki, and R. Watanabe, *Phys. Rev. D* **94**, 034001 (2016).
- [99] I. Dorner, S. Fajfer, A. Greljo, J. F. Kamenik, and N. Konik, *Phys. Rep.* **641**, 1 (2016).
- [100] I. de Medeiros Varzielas and G. Hiller, *J. High Energy Phys.* **06** (2015) 072.
- [101] I. Dorsner, J. Drobna, S. Fajfer, J. F. Kamenik, and N. Kosnik, *J. High Energy Phys.* **11** (2011) 002.
- [102] S. Davidson, D. C. Bailey, and B. A. Campbell, *Z. Phys. C* **61**, 613 (1994).
- [103] J. P. Saha, B. Misra, and A. Kundu, *Phys. Rev. D* **81**, 095011 (2010).
- [104] R. Mohanta, *Phys. Rev. D* **89**, 014020 (2014).
- [105] S. Sahoo and R. Mohanta, *New J. Phys.* **18**, 013032 (2016).
- [106] S. Sahoo and R. Mohanta, *Phys. Rev. D* **93**, 114001 (2016).
- [107] S. Sahoo and R. Mohanta, *Phys. Rev. D* **93**, 034018 (2016).
- [108] S. Sahoo and R. Mohanta, *Phys. Rev. D* **91**, 094019 (2015).
- [109] N. Kosnik, *Phys. Rev. D* **86**, 055004 (2012).
- [110] B. Chauhan, B. Kindra, and A. Narang, *Phys. Rev. D* **97**, 095007 (2018).
- [111] D. Beirevi, I. Dorner, S. Fajfer, N. Konik, D. A. Faroughy, and O. Sumensari, *Phys. Rev. D* **98**, 055003 (2018).
- [112] A. Angelescu, D. Beirevi, D. A. Faroughy, and O. Sumensari, *J. High Energy Phys.* **10** (2018) 183.
- [113] S. Sahoo and R. Mohanta, *Eur. Phys. J. C* **77**, 344 (2017).
- [114] S. Sahoo and R. Mohanta, *New J. Phys.* **18**, 093051 (2016).
- [115] S. Sahoo and R. Mohanta, *J. Phys. G* **44**, 035001 (2017).
- [116] S. Sahoo and A. Bhol, *arXiv:2005.12630*.
- [117] D. A. Faroughy, *SciPost Phys. Proc.* **1**, 021 (2019).
- [118] M. Napsuciale, S. Rodríguez, and H. Hernández-Arellano, *arXiv:2009.10658*.
- [119] A. Hook, E. Izaguirre, and J. G. Wacker, *Adv. High Energy Phys.* **2011**, 859762 (2011).
- [120] J. M. Cline, G. Dupuis, Z. Liu, and W. Xue, *J. High Energy Phys.* **08** (2014) 131.
- [121] J. P. Lees *et al.* (*BABAR* Collaboration), *Phys. Rev. D* **94**, 011102 (2016).
- [122] A. M. Sirunyan *et al.* (*CMS* Collaboration), *Phys. Lett. B* **792**, 345 (2019).
- [123] I. Adachi *et al.* (*Belle-II* Collaboration), *Phys. Rev. Lett.* **124**, 141801 (2020).
- [124] S. R. Mishra *et al.* (*CCFR* Collaboration), *Phys. Rev. Lett.* **66**, 3117 (1991).
- [125] W. Altmannshofer, S. Gori, M. Pospelov, and I. Yavin, *Phys. Rev. Lett.* **113**, 091801 (2014).
- [126] A. V. Semenov, *arXiv:hep-ph/9608488*.
- [127] A. Pukhov, E. Boos, M. Dubinin, V. Edneral, V. Ilyin, D. Kovalenko, A. Kryukov, V. Savrin, S. Shichanin, and A. Semenov, *arXiv:hep-ph/9908288*.
- [128] G. Belanger, F. Boudjema, A. Pukhov, and A. Semenov, *Comput. Phys. Commun.* **176**, 367 (2007).
- [129] G. Belanger, F. Boudjema, A. Pukhov, and A. Semenov, *Comput. Phys. Commun.* **180**, 747 (2009).
- [130] N. Aghanim *et al.* (*Planck* Collaboration), *Astron. Astrophys.* **641**, A6 (2020).
- [131] M. Aaboud *et al.* (*ATLAS* Collaboration), *Phys. Rev. Lett.* **122**, 231801 (2019).
- [132] S. Schael *et al.* (*ALEPH*, *DELPHI*, *L3*, *OPAL*, *SLD*, *LEP Electroweak Working Group*, *SLD Electroweak Group*, *SLD Heavy Flavour Group*), *Phys. Rep.* **427**, 257 (2006).
- [133] P. Agrawal, Z. Chacko, C. Kilic, and R. K. Mishra, *arXiv:1003.1912*.
- [134] R. Agnese *et al.* (*SuperCDMS* Collaboration), *Phys. Rev. D* **97**, 022002 (2018).
- [135] E. Ma, *Phys. Rev. D* **73**, 077301 (2006).
- [136] A. Vicente, *arXiv:1507.06349*.
- [137] C. Bobeth, M. Misiak, and J. Urban, *Nucl. Phys.* **B574**, 291 (2000).
- [138] C. Bobeth, A. J. Buras, F. Kruger, and J. Urban, *Nucl. Phys.* **B630**, 87 (2002).
- [139] W.-S. Hou, M. Kohda, and F. Xu, *Phys. Rev. D* **90**, 013002 (2014).
- [140] J. Hisano, T. Moroi, K. Tobe, and M. Yamaguchi, *Phys. Rev. D* **53**, 2442 (1996).
- [141] C. Bobeth, G. Hiller, and D. van Dyk, *J. High Energy Phys.* **07** (2011) 067.
- [142] B. Grinstein and D. Pirjol, *Phys. Rev. D* **70**, 114005 (2004).
- [143] C. Bobeth, G. Hiller, and D. van Dyk, *J. High Energy Phys.* **07** (2010) 098.

- [144] P. Colangelo, F. De Fazio, P. Santorelli, and E. Scrimieri, *Phys. Lett. B* **395**, 339 (1997).
- [145] C. Bobeth, G. Hiller, and G. Piranishvili, *J. High Energy Phys.* **07** (2008) 106.
- [146] W. Altmannshofer, P. Ball, A. Bharucha, A. J. Buras, D. M. Straub, and M. Wick, *J. High Energy Phys.* **01** (2009) 019.
- [147] P. Ball and R. Zwicky, *Phys. Rev. D* **71**, 014029 (2005).
- [148] M. Misiak *et al.*, *Phys. Rev. Lett.* **114**, 221801 (2015).
- [149] Y. Amhis *et al.* (HFLAV Collaboration), *Eur. Phys. J. C* **77**, 895 (2017).
- [150] B. Abi *et al.* (Muon g-2 Collaboration), *Phys. Rev. Lett.* **126**, 141801 (2021).
- [151] M. Misiak and J. Urban, *Phys. Lett. B* **451**, 161 (1999).
- [152] G. Buchalla and A. J. Buras, *Nucl. Phys.* **B548**, 309 (1999).
- [153] C. S. Kim, Y. G. Kim, and T. Morozumi, *Phys. Rev. D* **60**, 094007 (1999).